

# LHC phenomenology of the $\mu\nu$ SSM

A. Bartl\*

*Institut für Theoretische Physik, Universität Wien,  
A-1090 Vienna, Austria*

M. Hirsch<sup>†</sup> and A. Vicente<sup>‡</sup>

*AHEP Group, Institut de Física Corpuscular – C.S.I.C. & Universitat de València  
Edificio Institutos de Paterna, Apt 22085, E-46071 Valencia, Spain*

S. Liebler<sup>§</sup> and W. Porod<sup>¶</sup>

*Institut für Theoretische Physik und Astronomie, Universität Würzburg  
Am Hubland, D-97074 Würzburg, Germany*

The  $\mu\nu$ SSM has been proposed to solve simultaneously the  $\mu$ -problem of the MSSM and explain current neutrino data. The model breaks lepton number as well as R-parity. In this paper we study the phenomenology of this proposal concentrating on neutrino masses and the decay of the lightest supersymmetric particle (LSP). At first we investigate in detail the  $\mu\nu$ SSM with one generation of singlets, which can explain all neutrino data, once 1-loop corrections are taken into account. Then we study variations of the model with more singlets, which can generate all neutrino masses and mixings at tree-level. We calculate the decay properties of the lightest supersymmetric particle, assumed to be the lightest neutralino, taking into account all possible final states. The parameter regions where the LSP decays within the LHC detectors but with a length large enough to show a displaced vertex are identified. Decay branching ratios of certain final states show characteristic correlations with the measured neutrino angles, allowing to test the model at the LHC. Finally we briefly discuss possible signatures, which allow to distinguish between different R-parity breaking models.

## I. INTRODUCTION

The Minimal Supersymmetric extension of the Standard Model (MSSM) [1] assumes that R-parity is conserved. R-parity ( $R_p$ ) [2], defined as  $R_p = (-1)^{3B+L+2S}$ , was originally introduced to guarantee the stability of the proton in supersymmetric models [3, 4]. It has two immediate consequences: First, the lightest supersymmetric particle (LSP) is stable. For cosmological reasons a stable LSP has to be electrically neutral, thus leading to the “standard” missing momentum signature of SUSY. Second, the MSSM with  $R_p$ , for the same reasons as the SM, predicts zero neutrino masses.

Neutrino oscillation experiments have demonstrated that at least two neutrinos have non-zero mass [5, 6, 7]. Especially remarkable is that data from both atmospheric neutrino [8] and from reactor neutrino measurements [9] now show the characteristic  $L/E$  dependence expected from oscillations, ruling out or seriously disfavoring other explanations of the observed neutrino deficits. It is fair to say that with the most recent data by the KamLAND [9], Super-K [10] and MINOS collaborations [11] neutrino physics has finally entered the precision era. (For the latest evaluation of allowed neutrino parameter regions, see for example the updated fits in [12].)

---

\*Electronic address: alfred.bartl@univie.ac.at

<sup>†</sup>Electronic address: mahirsch@ific.uv.es

<sup>‡</sup>Electronic address: Avelino.Vicente@ific.uv.es

<sup>§</sup>Electronic address: sliebler@physik.uni-wuerzburg.de

<sup>¶</sup>Electronic address: porod@physik.uni-wuerzburg.de

Non-zero neutrino masses can be easily included into the standard model by simply adding right-handed neutrinos, postulating the existence of a ( $\Delta L = 2$ ) dimension-5 operator [13] of unspecified origin or by introducing the seesaw mechanism with either fermionic singlets [14, 15, 16], a scalar triplet [17, 18] or fermionic triplets [19]. Neutrino masses could be induced also at 1-loop-level [20] or even at 2-loop order [18, 21, 22].

While all of the neutrino mass models mentioned above can be easily supersymmetrized, there is also an entirely supersymmetric possibility to generate Majorana neutrino masses: R-parity violation [23, 24, 25]. Different models of (lepton number violating) R-parity violation have been discussed in the literature. Within the MSSM particle content R-parity can be broken explicitly either by bilinear or by trilinear terms [24]. The huge number of free parameters in the trilinear model, however, makes such a general ansatz rather arbitrary. Attempts to reduce the number of free parameters based on discrete symmetries have been discussed in the literature [26, 27, 28, 29]. One could also postulate that lepton number is conserved at the superpotential level, broken only by the vacuum expectation value (vev) of some singlet field [30]. This is called spontaneous R-parity violation ( $s\text{-}\mathcal{R}_p$ ).<sup>1</sup> Bilinear  $\mathcal{R}_p$  ( $b\text{-}\mathcal{R}_p$ ) can be understood as the low-energy limit of some  $s\text{-}\mathcal{R}_p$  model, where the new singlet fields are all decoupled. Such a bilinear model has only six new  $\mathcal{R}_p$  parameters and is thus more predictive than the general case with all possible bilinear and trilinear couplings.<sup>2</sup>

The phenomenology of  $\mathcal{R}_p$  SUSY has been studied extensively in the past, for reviews see [33, 34]. Neutrino masses have been calculated with trilinear couplings [24] and for pure bilinear models [35, 36, 37]. Neutrino angles are not predicted in either schemes, but can be easily fitted to experimental data. In bilinear schemes the requirement to correctly explain neutrino data fixes all  $\mathcal{R}_p$  couplings in sufficiently small intervals such that in some specific final states of the decays of the LSP correlations with neutrino angles appear. This has been shown for a (bino-dominated) neutralino LSP in [38], for charged scalar LSPs in [39] and for sneutrino, chargino, gluino and squark LSPs in [40]. Such a tight connection between neutrino physics and LSP decays is lost, however, in the general trilinear-plus-bilinear case. (For some recent work on collider phenomenology in trilinear  $\mathcal{R}_p$ , see for example [41, 42, 43, 44] and references in [33].)

The superpotential of the MSSM contains a mass term for the Higgs superfields,  $\mu \widehat{H}_d \widehat{H}_u$ . For phenomenological reasons this parameter  $\mu$  must be of the order of the electro-weak scale. However, if there is a larger scale in the theory, like the grand unification scale, the natural value of  $\mu$  lies at this large scale. This is, in short, the  $\mu$ -problem of the MSSM [45]. The Next-to-Minimal SSM (NMSSM) provides a solution to this problem [46, 47], at the cost of introducing a new singlet field. The vev of the singlet produces the  $\mu$  term, once electro-weak symmetry is broken. (For some recent papers on the phenomenology of the NMSSM, see for example [48, 49, 50] and references therein.)

The  $\mu\nu$ SSM [51] proposes to use the same singlet superfield(s) which generate the  $\mu$  term to also generate Dirac mass terms for the observed left-handed neutrinos. Lepton number in this approach is broken explicitly by cubic terms coupling only singlets.  $R_p$  is broken also and Majorana neutrino masses are generated once electro-weak symmetry is broken. Two recent papers have studied the  $\mu\nu$ SSM in more detail. In [52] the authors analyze the parameter space of the  $\mu\nu$ SSM, putting special emphasis on constraints arising from correct electro-weak symmetry breaking, avoiding tachyonic states and Landau poles in the parameters. The phenomenology of the  $\mu\nu$ SSM has been studied also in [53]. In this paper formulas for tree-level neutrino masses are given and decays of a neutralino LSP to two-body ( $W$ -lepton) final states have been calculated [53].

We note that similar proposals have been discussed in the literature. [54] studied a model in which the NMSSM singlet is coupled to (right-handed) singlet neutrino superfields. Effectively this leads to a model which is very similar to the NMSSM with explicit bilinear terms, as studied for example also in [55]. In [56] the authors propose a model similar to the  $\mu\nu$ SSM, but with only one singlet.

In the present paper, we study the phenomenology of the  $\mu\nu$ SSM, extending previous work [51, 52, 53]. We consider two different variations of the model. In its simplest form the  $\mu\nu$ SSM contains only one new singlet.

<sup>1</sup> The first model to propose  $s\text{-}\mathcal{R}_p$  [23] used the left-sneutrinos to break  $R_p$ . This leads to a doublet Majoron, now ruled out by LEP data [31].

<sup>2</sup> In [32] it has been proposed that the trilinear parameters follow the hierarchies of the standard model Yukawa couplings. This is very similar to the pure bilinear model, which in the mass eigenstate basis has effective trilinear parameters given by products of bilinear parameters and down quark/charged lepton Yukawa couplings.

This version produces one neutrino mass at tree-level, while the remaining two neutrinos receive mass at the loop-level. This feature is very similar to bilinear R-parity breaking, although as discussed below, the relative importance of the various loops is different for the explicit bilinear model and the  $\mu\nu$ SSM. As in the explicit bilinear model neutrino angles restrict the allowed range of  $\mathcal{R}_p$  parameters and correlations between certain ratios of decay branching ratios of the LSP and neutrino angles appear. In the second version we allow for  $n$  singlets. Neutrino masses can then be fitted with tree-level physics only. However, many of the features of the one generation model remain at least qualitatively also in the  $n$  singlet variants. LSP decays (for a bino or a singlino LSP) can be correlated with either the solar or atmospheric angle, thus allowing to construct explicit tests of the model for the LHC. In contrast to [53] we consider all kinematically allowed final states. This does not only cover scenarios where two-body decays are important, but also those where three-body decays are dominant. In addition we show that even in the scenarios where two-body decay modes in singlet Higgs bosons dominate, the lifetime can be such that the LSP decays outside the detector.

This paper is organized as follows. In the next section we outline the model, give the soft breaking terms, discuss the mass matrices and calculate approximate formulas for neutrino masses. We will not use the approximate formulas in our numerical analysis, but give them explicitly because they allow to understand in an easy way our numerical results qualitatively. In Section III we discuss existing constraints on the model space, apart from neutrino physics, and outline the properties of the “standard” points, which we will use in our numerical analysis. We then turn to the collider phenomenology of the model. In Section IV we study the one generation variant of the  $\mu\nu$ SSM. Decays of scalars are briefly discussed, before calculating decay properties of the neutralino LSP. Section V gives a discussion of the LSP phenomenology for the  $n$  generation variant, although we will mainly focus on two generations. Similarities and differences to the one generation model are discussed. In Section VI we then give a short, mostly qualitative discussion of possible signals which might give some hints which R-parity breaking model is indeed realized in nature, before closing with a short summary. Mass matrices and couplings are given in various appendices.

## II. MODEL BASICS

In this section we introduce the model, work out its most important properties related to phenomenology and neutrino masses and mixings. As explained in the introduction, we will consider the  $n$  generations case in this section. Approximate formulas are then given for scalar masses for the one (1)  $\hat{\nu}^c$ -model and for neutrino masses for the 1 and 2  $\hat{\nu}^c$ -model.

### A. Superpotential

The model contains  $n$  generations of right-handed neutrino singlets. The superpotential can be written as

$$\begin{aligned} \mathcal{W} = & h_U^{ij} \widehat{Q}_i \widehat{U}_j \widehat{H}_u + h_D^{ij} \widehat{Q}_i \widehat{D}_j \widehat{H}_d + h_E^{ij} \widehat{L}_i \widehat{E}_j \widehat{H}_d \\ & + h_\nu^{is} \widehat{L}_i \widehat{\nu}_s^c \widehat{H}_u - \lambda_s \widehat{\nu}_s^c \widehat{H}_d \widehat{H}_u + \frac{1}{3!} \kappa_{stu} \widehat{\nu}_s^c \widehat{\nu}_t^c \widehat{\nu}_u^c \quad . \end{aligned} \quad (1)$$

The last three terms include the right-handed neutrino superfields, which additionally play the role of the  $\widehat{\Phi}$  superfield in the NMSSM [46], a gauge singlet with respect to the SM gauge group. The model does not contain any terms with dimensions of mass, providing a natural solution to the  $\mu$ -problem of the MSSM. Please note, that as the number of right-handed neutrino superfields can be different from 3 we use the letters  $s$ ,  $t$  and  $u$  as generation indices for the  $\widehat{\nu}^c$  superfields and reserve the letter  $i$ ,  $j$  and  $k$  as generation indices for the usual MSSM matter fields.

The last two terms in (1) explicitly break lepton number and thus R-parity giving rise to neutrino masses. Note that  $\kappa_{stu}$  is completely symmetric in all its indices. In contrast to other models with R-parity violation, this model does not need the presence of unnaturally small parameters with dimensions of mass, like in bilinear R-parity breaking models [34], and there is no Goldstone boson associated with the breaking of lepton number [23, 57, 58], since breaking of  $R_p$  is done explicitly.

For practical purposes, it is useful to write the superpotential in the basis where the right-handed neutrinos have a diagonal mass matrix. Since their masses are induced by the  $\kappa$  term in (1), this is equivalent to writing this term including only diagonal couplings:

$$\kappa_{stu} \widehat{\nu}_s^c \widehat{\nu}_t^c \widehat{\nu}_u^c \quad \Longrightarrow \quad \sum_{s=1}^n \kappa_s (\widehat{\nu}_s^c)^3 \quad (2)$$

## B. Soft terms

The soft SUSY breaking terms of the model are

$$V_{soft} = V_{soft}^{MSSM-B_\mu} + V_{soft}^{singlets} \quad . \quad (3)$$

$V_{soft}^{MSSM-B_\mu}$  contains all the usual soft terms of the MSSM but the  $B_\mu$ -term

$$\begin{aligned} V_{soft}^{MSSM-B_\mu} &= m_Q^{ij2} \tilde{Q}_i^{a*} \tilde{Q}_j^a + m_U^{ij2} \tilde{U}_i \tilde{U}_j^* + m_D^{ij2} \tilde{D}_i \tilde{D}_j^* + m_L^{ij2} \tilde{L}_i^{a*} \tilde{L}_j^a + m_E^{ij2} \tilde{E}_i \tilde{E}_j^* \\ &+ m_{H_d}^2 H_d^{a*} H_d^a + m_{H_u}^2 H_u^{a*} H_u^a - \frac{1}{2} [M_1 \tilde{B}^0 \tilde{B}^0 + M_2 \tilde{W}^c \tilde{W}^c + M_3 \tilde{g}^d \tilde{g}^d + h.c.] \\ &+ \epsilon_{ab} [T_U^{ij} \tilde{Q}_i^a \tilde{U}_j^* H_u^b + T_D^{ij} \tilde{Q}_i^b \tilde{D}_j^* H_d^a + T_E^{ij} \tilde{L}_i^b \tilde{E}_j^* H_d^a + h.c.] \end{aligned} \quad (4)$$

and  $V_{soft}^{singlets}$  includes the new terms with singlets:

$$V_{soft}^{singlets} = m_{\tilde{\nu}^c}^{st2} \tilde{\nu}_s^c \tilde{\nu}_t^{c*} + \epsilon_{ab} [T_{h_\nu}^{st} \tilde{L}_s^a \tilde{\nu}_t^c H_u^b - T_\lambda^s \tilde{\nu}_s^c H_d^a H_u^b + h.c.] + \left[ \frac{1}{3!} T_\kappa^{stu} \tilde{\nu}_s^c \tilde{\nu}_t^c \tilde{\nu}_u^c + h.c. \right] \quad (5)$$

In these expressions the notation for the soft trilinear couplings introduced in [59, 60] is used. Note that the rotation made in the superpotential does not necessarily diagonalize the soft trilinear terms  $T_\kappa^{stu}$  implying in general additional mixing between the right-handed sneutrinos.

## C. Scalar potential and its minimization

Summing up the different contributions, the scalar potential considering only neutral fields reads

$$V = V_D + V_F + V_{soft} \quad (6)$$

with

$$V_D = \frac{1}{8} (g^2 + g'^2) (|H_u^0|^2 - |H_d^0|^2 - \sum_{i=1}^3 |\tilde{\nu}_i|^2)^2 \quad (7)$$

$$V_F = |h_\nu^{is} \tilde{\nu}_i \tilde{\nu}_s^c - \lambda_s \tilde{\nu}_s^c H_d^0|^2 + |\lambda_s \tilde{\nu}_s^c H_u^0|^2 + \sum_{i=1}^3 |h_\nu^{is} \tilde{\nu}_i \tilde{\nu}_s^c H_u^0|^2 + \sum_{s=1}^n |h_\nu^{is} \tilde{\nu}_i H_u^0 - \lambda_s H_u^0 H_d^0 + \frac{1}{2} \kappa_s (\tilde{\nu}_s^c)^2|^2 \quad , \quad (8)$$

where summation over repeated indices is implied.

This scalar potential determines the structure of the vacuum, inducing vevs:

$$\langle H_d^0 \rangle = \frac{v_d}{\sqrt{2}}, \quad \langle H_u^0 \rangle = \frac{v_u}{\sqrt{2}}, \quad \langle \tilde{\nu}_s^c \rangle = \frac{v_{R_s}}{\sqrt{2}}, \quad \langle \tilde{\nu}_i \rangle = \frac{v_i}{\sqrt{2}} \quad (9)$$

In particular, the vevs for the right-handed sneutrinos generate effective bilinear couplings:

$$h_\nu^{is} \widehat{L}_i \widehat{\nu}_s^c \widehat{H}_u - \lambda_s \widehat{\nu}_s^c \widehat{H}_d \widehat{H}_u \quad \Longrightarrow \quad h_\nu^{is} \widehat{L}_i \frac{v_{R_s}}{\sqrt{2}} \widehat{H}_u - \lambda_s \frac{v_{R_s}}{\sqrt{2}} \widehat{H}_d \widehat{H}_u \equiv \epsilon_i \widehat{L}_i \widehat{H}_u - \mu \widehat{H}_d \widehat{H}_u \quad (10)$$

Since by electroweak symmetry breaking an effective  $\mu$  term is generated, it is at the electroweak scale. Minimizing the scalar potential gives the following tadpole equations at tree-level

$$\begin{aligned} \frac{\partial V}{\partial v_d} &= \frac{1}{8}(g^2 + g'^2)u^2 v_d + m_{H_d}^2 v_d + \frac{1}{2}v_d \lambda_s \lambda_t^* v_{Rs} v_{Rt} + \frac{1}{2}v_d v_u^2 \lambda_s \lambda_s^* \\ &\quad - \frac{1}{8}v_{Rs}^2 v_u (\kappa_s \lambda_s^* + h.c.) - \frac{1}{4}v_i (\lambda_s^* h_\nu^{it} v_{Rs} v_{Rt} + h.c.) - \frac{1}{4}v_u^2 v_i (\lambda_s^* h_\nu^{is} + h.c.) \\ &\quad - \frac{1}{2\sqrt{2}}v_u v_{Rs} (T_\lambda^s + h.c.) = 0 \end{aligned} \quad (11)$$

$$\begin{aligned} \frac{\partial V}{\partial v_u} &= -\frac{1}{8}(g^2 + g'^2)u^2 v_u + m_{H_u}^2 v_u + \frac{1}{2}v_u \lambda_s \lambda_t^* v_{Rs} v_{Rt} + \frac{1}{2}v_d^2 v_u \lambda_s \lambda_s^* - \frac{1}{8}v_{Ri}^2 v_d (\kappa_s \lambda_s^* + h.c.) \\ &\quad + \frac{1}{8}v_i v_{Rs}^2 (\kappa_s^* h_\nu^{is} + h.c.) - \frac{1}{2}v_d v_u v_i (\lambda_s^* h_\nu^{is} + h.c.) + \frac{1}{2}v_u v_i v_j h_\nu^{is} (h_\nu^{js})^* \\ &\quad + \frac{1}{2}v_u h_\nu^{is} (h_\nu^{it})^* v_{Rs} v_{Rt} - \frac{1}{2\sqrt{2}}v_d v_{Rs} (T_\lambda^s + h.c.) + \frac{1}{2\sqrt{2}}v_i v_{Rs} (T_{h_\nu}^{is} + h.c.) = 0 \end{aligned} \quad (12)$$

$$\begin{aligned} \frac{\partial V}{\partial v_i} &= \frac{1}{8}(g^2 + g'^2)u^2 v_i + \frac{1}{2}(m_{L_{ij}}^2 + m_{L_{ji}}^2)v_j - \frac{1}{4}v_d v_u^2 (\lambda_s^* h_\nu^{is} + h.c.) \\ &\quad + \frac{1}{8}v_{Rs}^2 v_u (\kappa_s^* h_\nu^{is} + h.c.) - \frac{1}{4}v_d (\lambda_s^* v_{Rs} v_{Rt} h_\nu^{it} + h.c.) + \frac{1}{4}v_j (v_{Rs} v_{Rt} h_\nu^{is} (h_\nu^{jt})^* + h.c.) \\ &\quad + \frac{1}{4}v_u^2 v_j (h_\nu^{is} (h_\nu^{js})^* + h.c.) + \frac{1}{2\sqrt{2}}v_u v_{Rs} (T_{h_\nu}^{is} + h.c.) = 0 \end{aligned} \quad (13)$$

$$\begin{aligned} \frac{\partial V}{\partial v_{Rs}} &= m_{\tilde{\nu}^c s s}^2 v_{Rs} - \frac{1}{4}v_d v_u v_{Rs} (\kappa_s \lambda_s^* + h.c.) + \frac{1}{4}\kappa_s \kappa_s^* v_{Rs}^3 \\ &\quad + \frac{1}{4}v_u v_{Rs} v_j (\kappa_s^* h_\nu^{js} + h.c.) + \frac{1}{4}(v_u^2 + v_d^2)(\lambda_s \lambda_t^* v_{Rt} + h.c.) + \frac{1}{4}v_u^2 [h_\nu^{js} (h_\nu^{jt})^* v_{Rt} + h.c.] \\ &\quad + \frac{1}{4}v_m v_n [(h_\nu^{ms})^* h_\nu^{nt} v_{Rt} + h.c.] - \frac{1}{4}v_d v_j (\lambda_t^* h_\nu^{js} v_{Rt} + \lambda_s^* v_{Rt} h_\nu^{jt} + h.c.) \\ &\quad - \frac{1}{2\sqrt{2}}v_d v_u (T_\lambda^s + h.c.) + \frac{1}{2\sqrt{2}}v_u v_j (T_{h_\nu}^{js} + h.c.) + \frac{1}{4\sqrt{2}}v_{Rt} v_{Ru} (T_\kappa^{stu} + h.c.) = 0 \end{aligned} \quad (14)$$

with

$$u^2 = v_d^2 - v_u^2 + v_1^2 + v_2^2 + v_3^2 \quad (15)$$

and there is no sum over the index  $s$  in Equation (14).

As usual in R-parity breaking models with right-handed neutrinos, see for example the model proposed in [30], it is possible to explain the smallness of the  $v_i$  in terms of the smallness of the Yukawa couplings  $h_\nu$ , that generate Dirac masses for the neutrinos. This can be easily seen from Equation (13), where both quantities are proportional. Moreover, as shown in [51], taking the limit  $h_\nu \rightarrow 0$  and, consequently,  $v_i \rightarrow 0$ , one recovers the tadpole equations of the NMSSM, ensuring the existence of solutions to this set of equations.

#### D. Masses of the neutral scalars and pseudoscalars

In this subsection we work out the main features of the neutral scalar sector mainly focusing on singlets. The complete mass matrices are given in Appendix A. We start with the one generation case which closely resembles the NMSSM, considered, for example, in [61, 62]. This already implies an upper bound on the lightest doublet Higgs mass  $m(h^0)$ , where we will focus on at the end of this subsection. A correct description of neutrino physics implies small values for the vevs  $v_i$  of the left sneutrinos and small Yukawa couplings  $h_\nu$  as we will see later. Neglecting mixing terms proportional to these quantities, the  $(6 \times 6)$  mass matrix of the pseudoscalars in the basis  $Im(H_d^0, H_u^0, \tilde{\nu}^c, \tilde{\nu}_i)$  given in Appendix A, Equation (A20), can be decomposed in

two  $(3 \times 3)$  blocks. By using the tadpole equations we obtain

$$M_{P_0}^2 = \begin{pmatrix} M_{HH}^2 & M_{HS}^2 & 0 \\ (M_{HS}^2)^T & M_{SS}^2 & 0 \\ 0 & 0 & M_{\tilde{L}\tilde{L}}^2 \end{pmatrix} \quad (16)$$

with

$$M_{HH}^2 = \begin{pmatrix} (\Omega_1 + \Omega_2) \frac{v_u}{v_d} & \Omega_1 + \Omega_2 \\ \Omega_1 + \Omega_2 & (\Omega_1 + \Omega_2) \end{pmatrix}, \quad M_{HS}^2 = \begin{pmatrix} (-2\Omega_1 + \Omega_2) \frac{v_u}{v_R} \\ (-2\Omega_1 + \Omega_2) \frac{v_d}{v_R} \end{pmatrix}$$

$$M_{SS}^2 = (4\Omega_1 + \Omega_2) \frac{v_d v_u}{v_R^2} - 3\Omega_3, \quad (M_{\tilde{L}\tilde{L}}^2)_{ij} = \frac{1}{2} (m_{\tilde{L}}^2)_{ij} + \frac{1}{2} (m_{\tilde{L}}^2)_{ji} + \delta_{ij} \left[ \frac{1}{8} (g^2 + g'^2) u^2 \right], \quad (17)$$

where  $u^2$  is defined in Equation (15). The parameters  $\Omega_i$  are defined as:

$$\Omega_1 = \frac{1}{8} (\lambda \kappa^* + \lambda^* \kappa) v_R^2, \quad \Omega_2 = \frac{1}{2\sqrt{2}} (T_\lambda + T_\lambda^*) v_R, \quad \Omega_3 = \frac{1}{4\sqrt{2}} (T_\kappa + T_\kappa^*) v_R \quad (18)$$

The upper  $(3 \times 3)$  block contains the mass terms for  $Im(H_d)$ ,  $Im(H_u)$  and  $Im(\tilde{\nu}^c)$  and we get analytic expressions for the eigenvalues:

$$m^2(P_1^0) = 0$$

$$m^2(P_2^0) = \frac{1}{2} (\Omega_1 + \Omega_2) \left( \frac{v_d}{v_u} + \frac{v_u}{v_d} + \frac{v_d v_u}{v_R^2} \right) - \frac{3}{2} \Omega_3 - \sqrt{\Gamma}$$

$$m^2(P_3^0) = \frac{1}{2} (\Omega_1 + \Omega_2) \left( \frac{v_d}{v_u} + \frac{v_u}{v_d} + \frac{v_d v_u}{v_R^2} \right) - \frac{3}{2} \Omega_3 + \sqrt{\Gamma}$$

$$\text{with } \Gamma = \left( \frac{1}{2} (\Omega_1 + \Omega_2) \left( \frac{v_d}{v_u} + \frac{v_u}{v_d} + \frac{v_d v_u}{v_R^2} \right) - \frac{3}{2} \Omega_3 \right)^2$$

$$+ 3 (\Omega_1 + \Omega_2) \Omega_3 \left( \frac{v_d}{v_u} + \frac{v_u}{v_d} \right) - 9\Omega_1 \Omega_2 \left( \frac{v_R^2}{v_d^2} + \frac{v_R^2}{v_u^2} \right) \quad (19)$$

The first eigenvalue corresponds to the Goldstone boson due to spontaneous symmetry breaking. To get only positive eigenvalues for the physical states, the condition

$$\Omega_3 < \frac{v_d v_u}{v_R^2} \frac{3\Omega_1 \Omega_2}{\Omega_1 + \Omega_2} =: f_1(\Omega_2) \quad (20)$$

has to be fulfilled, implying that  $T_\kappa$  has in general the opposite sign of  $v_R$ . Additional constraints on the parameters are obtained from the positiveness of the squared masses of the neutral scalars. Taking the scalar mass matrix from Appendix A, Equation (A11), in the basis  $Re(H_d^0, H_u^0, \tilde{\nu}^c, \tilde{\nu}_i)$  in the same limit as above we obtain

$$M_{S_0}^2 = \begin{pmatrix} M_{HH}^2 & M_{HS}^2 & 0 \\ (M_{HS}^2)^T & M_{SS}^2 & 0 \\ 0 & 0 & M_{\tilde{L}\tilde{L}}^2 \end{pmatrix} \quad (21)$$

with

$$M_{HH}^2 = \begin{pmatrix} (\Omega_1 + \Omega_2) \frac{v_u}{v_d} + \Omega_6 \frac{v_d}{v_u} & -\Omega_1 - \Omega_2 - \Omega_6 + \Omega_4 \\ -\Omega_1 - \Omega_2 - \Omega_6 + \Omega_4 & (\Omega_1 + \Omega_2) \frac{v_d}{v_u} + \Omega_6 \frac{v_u}{v_d} \end{pmatrix}, \quad M_{HS}^2 = \begin{pmatrix} (-2\Omega_1 - \Omega_2) \frac{v_u}{v_R} + \Omega_4 \frac{v_R}{v_d} \\ (-2\Omega_1 - \Omega_2) \frac{v_d}{v_R} + \Omega_4 \frac{v_R}{v_u} \end{pmatrix}$$

$$M_{SS}^2 = \Omega_2 \frac{v_d v_u}{v_R^2} + \Omega_3 + \Omega_5, \quad (M_{\tilde{L}\tilde{L}}^2)_{ij} = \frac{1}{4} (g^2 + g'^2) v_i v_j + \frac{1}{2} (m_{\tilde{L}}^2)_{ij} + \frac{1}{2} (m_{\tilde{L}}^2)_{ji} + \delta_{ij} \left[ \frac{1}{8} (g^2 + g'^2) u^2 \right] \quad (22)$$

using the additional parameters

$$\Omega_4 = \lambda \lambda^* v_d v_u > 0, \quad \Omega_5 = \frac{1}{2} \kappa \kappa^* v_R^2 > 0, \quad \Omega_6 = \frac{1}{4} (g^2 + g'^2) v_d v_u > 0 \quad . \quad (23)$$

An analytic determination of the eigenvalues is possible but not very illuminating. However, one can use the following theorem: A symmetric matrix is positive definite, if all eigenvalues are positive and this is equal to the positiveness of all principal minors (Sylvester criterion). This results in the following three conditions

$$\begin{aligned} 0 &< (\Omega_1 + \Omega_2) \frac{v_u}{v_d} + \Omega_6 \frac{v_d}{v_u} \\ 0 &< (\Omega_1 + \Omega_2) \left( \Omega_6 \left( \frac{v_d^2}{v_u^2} + \frac{v_u^2}{v_d^2} \right) - 2\Omega_6 + 2\Omega_4 \right) + 2\Omega_4 \Omega_6 - \Omega_4^2 \\ 0 &< \Omega_3 - f_2(\Omega_2) \quad , \end{aligned} \quad (24)$$

where  $f_2(\Omega_2)$  is given by:

$$\begin{aligned} f_2(\Omega_2) &= \frac{\Sigma_1}{\Sigma_2} \quad \text{with} \\ \Sigma_1 &= (\Omega_1 + \Omega_2) \Omega_5 (-2\Omega_4 + 2\Omega_6) + (\Omega_4^2 - 2\Omega_4 \Omega_6) \Omega_5 \\ &+ (\Omega_1 + \Omega_2) \Omega_4^2 v_R^2 \left( \frac{v_d}{v_u^3} + \frac{v_u}{v_d^3} \right) + (4\Omega_1^2 + 3\Omega_1 \Omega_2) \Omega_6 \frac{1}{v_R^2} \left( \frac{v_d^3}{v_u} + \frac{v_u^3}{v_d} \right) \\ &- (\Omega_1 + \Omega_2) \Omega_5 \Omega_6 \left( \frac{v_d^2}{v_u^2} + \frac{v_u^2}{v_d^2} \right) + 2(\Omega_1 + \Omega_2 - \Omega_4 + 2\Omega_6) \Omega_4^2 \frac{v_R^2}{v_d v_u} \\ &- 2(2\Omega_1 + \Omega_2) (2\Omega_1 + 2\Omega_2 - \Omega_4 + 2\Omega_6) \Omega_4 \left( \frac{v_d}{v_u} + \frac{v_u}{v_d} \right) \\ &+ [16\Omega_1^3 + 8(4\Omega_2 - \Omega_4 + \Omega_6) \Omega_1^2 + 10\Omega_1 \Omega_2 (2\Omega_2 - \Omega_4 + \Omega_6) \\ &+ \Omega_2 (2\Omega_2 - \Omega_4) (2\Omega_2 - \Omega_4 + 2\Omega_6)] \frac{v_d v_u}{v_R^2} \\ \Sigma_2 &= (\Omega_1 + \Omega_2) \Omega_6 \left( \frac{v_d^2}{v_u^2} + \frac{v_u^2}{v_d^2} \right) + 2(\Omega_1 + \Omega_2) (\Omega_4 - \Omega_6) \\ &+ 2\Omega_4 \Omega_6 - \Omega_4^2 \end{aligned} \quad (25)$$

The first two conditions are in general fulfilled, but for special values of  $\tan \beta$  or  $\lambda$ . Putting all the above together we get the following conditions:

$$f_2(\Omega_2) < \Omega_3 < f_1(\Omega_2) \quad (26)$$

It turns out that by taking a negative value of  $\Omega_3$  ( $\propto T_\kappa$ ) near  $f_2(\Omega_2)$  one obtains a very light singlet scalar, whereas for a value of  $\Omega_3$  near  $f_1(\Omega_2)$  one gets a very light singlet pseudoscalar. In between one finds a value of  $\Omega_3$ , where both particles have the same mass. This discussion is comparable to formula (37) in [62] for the NMSSM. Moreover, a small mass of the singlet scalar and/or pseudoscalar comes always together with a small mass of the singlet fermion.

In the  $n$  generation case similar result holds as long as  $T_\kappa$  and  $m_{\tilde{\nu}^c}^2$  do not have off-diagonal entries compared to  $\kappa$ . Inspecting Equations (A15) and (A24) it is possible to show that the singlet scalars and pseudoscalars can be heavy by appropriately chosen values for the off-diagonal entries of  $T_\kappa$  while keeping at the same time the singlet fermions relatively light, as will be discussed later. As pointed out in [52], the NMSSM upper bound on the lightest doublet Higgs mass of about  $\sim 150$  GeV, which also applies in the  $\mu\nu$ SSM, can be relaxed to  $\mathcal{O}(300)$  GeV, if one does not require perturbativity up to the GUT scale.

## E. Neutrino masses

In the basis

$$(\psi^0)^T = (\tilde{B}^0, \tilde{W}_3^0, \tilde{H}_d^0, \tilde{H}_u^0, \nu_s^c, \nu_i) \quad (27)$$

the mass matrix of the neutral fermions, see Appendix A 4, has the structure

$$\mathcal{M}_n = \begin{pmatrix} \mathbf{M}_H & \mathbf{m} \\ \mathbf{m}^T & \mathbf{0} \end{pmatrix} . \quad (28)$$

Here  $\mathbf{M}_H$  is the submatrix including the heavy states, which consists of the usual four neutralinos of the MSSM and  $n$  generations of right-handed neutrinos. The matrix  $\mathbf{m}$  mixes the heavy states with the left-handed neutrinos and contains the R-parity breaking parameters.

The matrix  $\mathcal{M}_n$  can be diagonalized in the standard way:

$$\widehat{\mathcal{M}}_n = \mathcal{N}^* \mathcal{M}_n \mathcal{N}^{-1} \quad (29)$$

As it is well known, the smallness of neutrino masses allows to find the effective neutrino mass matrix in a seesaw approximation

$$\mathbf{m}_{\nu\nu}^{\text{eff}} = -\mathbf{m}^T \cdot \mathbf{M}_H^{-1} \mathbf{m} = -\xi \cdot \mathbf{m} \quad , \quad (30)$$

where the matrix  $\xi$  contains the small expansion parameters which characterize the mixing between the neutrino sector and the heavy states.

Since the superpotential explicitly breaks lepton number, at least one mass for the left-handed neutrinos is generated at tree-level. In the case of the 1  $\hat{\nu}^c$ -model the other neutrino masses are generated at loop-level. With more than one generation of right-handed neutrinos additional neutrino masses are generated at tree-level, resulting in different possibilities to fit the neutrino oscillation data, see the discussion below.

### 1. One generation of right-handed neutrinos

With only one generation of right-handed neutrinos the matrix  $\xi$  is given by

$$\xi_{ij} = K_\Lambda^j \Lambda_i - \frac{1}{\mu} \epsilon_i \delta_{j3} \quad , \quad (31)$$

where the  $\epsilon_i$  and  $\Lambda_i$  parameters are defined as

$$\epsilon_i = \frac{1}{\sqrt{2}} h_\nu^i v_R \quad (32)$$

$$\Lambda_i = \mu v_i + \epsilon_i v_d \quad (33)$$

and  $K_\Lambda^j$  as

$$\begin{aligned} K_\Lambda^1 &= \frac{2g' M_2 \mu}{m_\gamma} a \\ K_\Lambda^2 &= -\frac{2g M_1 \mu}{m_\gamma} a \\ K_\Lambda^3 &= \frac{m_\gamma}{8\mu \text{Det}(M_H)} (\lambda^2 v_d v^2 + 2M_R \mu v_u) \\ K_\Lambda^4 &= -\frac{m_\gamma}{8\mu \text{Det}(M_H)} (\lambda^2 v_u v^2 + 2M_R \mu v_d) \\ K_\Lambda^5 &= \frac{\lambda m_\gamma}{4\sqrt{2} \text{Det}(M_H)} (v_u^2 - v_d^2) \end{aligned} \quad (34)$$

with

$$m_\gamma = g^2 M_1 + g'^2 M_2, \quad v^2 = v_d^2 + v_u^2, \quad M_R = \frac{1}{\sqrt{2}} \kappa v_R \quad (35)$$

$$a = \frac{m_\gamma}{4\mu \text{Det}(M_H)} (v_d v_u \lambda^2 + M_R \mu) \quad (36)$$



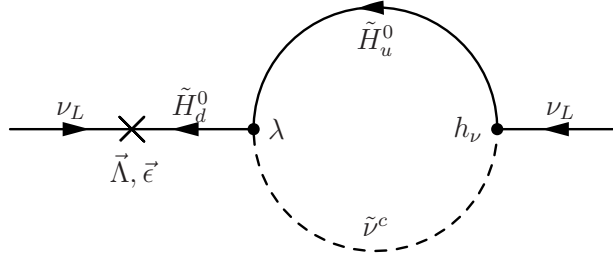


Figure 1: Example of one 1-loop correction to the effective neutrino mass matrix involving the singlet scalar/pseudoscalar.

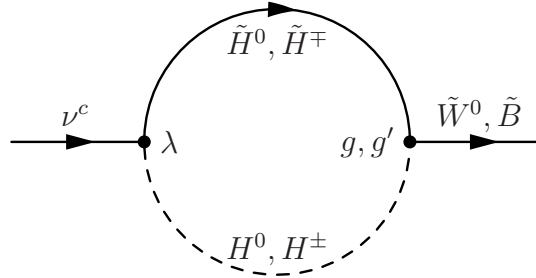


Figure 2: 1-loop mixing between gauginos and the right-handed neutrinos.

and  $\text{Det}(M_H)$  is the determinant of the  $(5 \times 5)$  mass matrix of the heavy states

$$\text{Det}(M_H) = \frac{1}{8}m_\gamma(\lambda^2 v^4 + 4M_R \mu v_d v_u) - M_1 M_2 \mu(v_d v_u \lambda^2 + M_R \mu) \quad . \quad (37)$$

Using these expressions the tree-level effective neutrino mass matrix takes the form

$$(\mathbf{m}_{\nu\nu}^{\text{eff}})_{ij} = a\Lambda_i\Lambda_j \quad . \quad (38)$$

The projective form of this mass matrix implies that only one neutrino gets a tree-level mass, while the other two remain massless. Therefore, as in models with bilinear R-parity violation [36, 37, 63] 1-loop corrections are needed in order to correctly explain the oscillation data, which require at least one additional massive neutrino. The absolute scale of neutrino mass constrains the  $\vec{\Lambda}$  and  $\vec{\epsilon}$  parameters, which have to be small. For typical SUSY masses order  $\mathcal{O}(100 \text{ GeV})$ , one finds  $|\vec{\Lambda}|/\mu^2 \sim 10^{-7}-10^{-6}$  and  $|\vec{\epsilon}|/\mu \sim 10^{-5}-10^{-4}$ . This implies a ratio of  $|\vec{\epsilon}|^2/|\vec{\Lambda}| \sim 10^{-3}-10^{-1}$ .

General formulas for the 1-loop contributions can be found in [36] and adjusted to the  $\mu\nu\text{SSM}$  with appropriate changes in the index ranges for neutralinos and scalars. Important contributions to the neutrino mass matrix are due to  $b - \tilde{b}$  and  $\tau - \tilde{\tau}$  loops as in the models with  $b\text{-}\tilde{R}_p$  [37]. In addition there are two new important contributions: (i) loops containing the singlet scalar and singlet pseudoscalar shown in Figure 1. As shown in [64, 65, 66], the sum of both contributions is proportional to the squared mass difference  $\Delta_{12} = m_R^2 - m_I^2 \propto \kappa^2 v_R^2$  between the singlet scalar and pseudoscalar mass eigenstates. Note that this splitting can be much larger than the corresponding ones for the left sneutrinos. Thus the sum of both loops can be more important than  $b - \tilde{b}$  and  $\tau - \tilde{\tau}$  loops in the current model. (ii) At loop-level a direct mixing between the right-handed neutrinos and the gauginos is possible which is zero at tree-level, see Figure 2.

2.  $n$  generations of right-handed neutrinos

In this class of models with  $n > 1$  one can explain the neutrino data using the tree-level neutrino mass matrix only. In general one finds that the loop corrections are small if the conditions at the end of this section are fulfilled.

For the sake of simplicity, let us consider two generations of right-handed neutrinos which contains all relevant features. The matrix  $\xi$  in Equation (30) takes the form

$$\xi_{ij} = K_{\Lambda}^j \Lambda_i + K_{\alpha}^j \alpha_i - \frac{\epsilon_i}{\mu} \delta_{j3} \quad (39)$$

with

$$\epsilon_i = \frac{1}{\sqrt{2}} h_{\nu}^{is} v_{Rs} \quad (40)$$

$$\Lambda_i = \mu v_i + \epsilon_i v_d \quad (41)$$

$$\alpha_i = v_u (\lambda_2 h_{\nu}^{i1} - \lambda_1 h_{\nu}^{i2}) \quad (42)$$

The  $K_{\Lambda}$  and  $K_{\alpha}$  coefficients are:

$$\begin{aligned} K_{\Lambda}^1 &= \frac{2g' M_2 \mu}{m_{\gamma}} a, & K_{\alpha}^1 &= \frac{2g' M_2 \mu}{m_{\gamma}} b \\ K_{\Lambda}^2 &= -\frac{2g M_1 \mu}{m_{\gamma}} a, & K_{\alpha}^2 &= -\frac{2g M_1 \mu}{m_{\gamma}} b \\ K_{\Lambda}^3 &= \frac{m_{\gamma}}{8\mu \text{Det}(M_H)} [v_d v^2 (M_{R1} \lambda_2^2 + M_{R2} \lambda_1^2) + 2v_u M_{R1} M_{R2} \mu], & K_{\alpha}^3 &= \frac{b}{m_{\gamma} (v_u^2 - v_d^2)} (m_{\gamma} v^2 v_u - 4M_1 M_2 \mu v_d) \\ K_{\Lambda}^4 &= -\frac{m_{\gamma}}{8\mu \text{Det}(M_H)} [v_u v^2 (M_{R1} \lambda_2^2 + M_{R2} \lambda_1^2) + 2v_d M_{R1} M_{R2} \mu], & K_{\alpha}^4 &= \frac{b}{m_{\gamma} (v_u^2 - v_d^2)} (m_{\gamma} v^2 v_d - 4M_1 M_2 \mu v_u) \\ K_{\Lambda}^5 &= \frac{M_{R2} \lambda_1 m_{\gamma}}{4\sqrt{2} \text{Det}(M_H)} (v_u^2 - v_d^2), & K_{\alpha}^5 &= -\sqrt{2} \lambda_2 c - \frac{4 \text{Det}_0 v_{R1}}{\mu m_{\gamma} (v_u^2 - v_d^2)} b \\ K_{\Lambda}^6 &= \frac{M_{R1} \lambda_2 m_{\gamma}}{4\sqrt{2} \text{Det}(M_H)} (v_u^2 - v_d^2), & K_{\alpha}^6 &= \sqrt{2} \lambda_1 c - \frac{4 \text{Det}_0 v_{R2}}{\mu m_{\gamma} (v_u^2 - v_d^2)} b \end{aligned} \quad (43)$$

The effective neutrino mass matrix reads as

$$(\mathbf{m}_{\nu\nu}^{\text{eff}})_{ij} = a \Lambda_i \Lambda_j + b (\Lambda_i \alpha_j + \Lambda_j \alpha_i) + c \alpha_i \alpha_j \quad (44)$$

with

$$a = \frac{m_{\gamma}}{4\mu \text{Det}(M_H)} (M_{R1} \lambda_2^2 v_u v_d + M_{R2} \lambda_1^2 v_u v_d + M_{R1} M_{R2} \mu) \quad (45)$$

$$b = \frac{m_{\gamma}}{8\sqrt{2}\mu \text{Det}(M_H)} (v_u^2 - v_d^2) (M_{R1} v_{R1} \lambda_2 - M_{R2} v_{R2} \lambda_1) \quad (46)$$

$$c = -\frac{1}{16\mu^2 \text{Det}(M_H)} [\mu^2 (m_{\gamma} v^4 - 8M_1 M_2 \mu v_u v_d) + 4 \text{Det}_0 (M_{R1} v_{R1}^2 + M_{R2} v_{R2}^2)] \quad (47)$$

using  $M_{Rs} = \frac{1}{\sqrt{2}} \kappa_s v_{Rs}$  and the determinant of the  $(6 \times 6)$  mass matrix of the heavy states is

$$\text{Det}(M_H) = \frac{1}{8} [(M_{R2} \lambda_1^2 + M_{R1} \lambda_2^2) (m_{\gamma} v^4 - 8M_1 M_2 \mu v_u v_d) + 8M_{R1} M_{R2} \text{Det}_0] \quad (48)$$

with  $\text{Det}_0$  being the determinant of the usual MSSM neutralino mass matrix

$$\text{Det}_0 = \frac{1}{2} m_{\gamma} \mu v_d v_u - M_1 M_2 \mu^2 \quad (49)$$

The mass matrix in Equation (44) has two nonzero eigenvalues and therefore the loop corrections are not needed to explain the experimental data. Two different options arise:

- $\vec{\Lambda}$  generates the atmospheric mass scale,  $\vec{\alpha}$  the solar mass scale
- $\vec{\alpha}$  generates the atmospheric mass scale,  $\vec{\Lambda}$  the solar mass scale

In both cases one obtains in general a hierarchical spectrum. A strong fine-tuning would be necessary to generate an inverted hierarchy which is not stable against small variations of the parameters or radiative corrections. Moreover the absolute scale of neutrino mass requires both  $|\vec{\Lambda}|/\mu^2$  and  $|\vec{\alpha}|/\mu$  to be small. For typical SUSY masses order  $\mathcal{O}(100 \text{ GeV})$  we find in the first case  $|\vec{\Lambda}|/\mu^2 \sim 10^{-7}-10^{-6}$  and  $|\vec{\alpha}|/\mu \sim 10^{-9}-10^{-8}$ . In the second case we find  $|\vec{\Lambda}|/\mu^2 \sim 10^{-8}-10^{-7}$  and  $|\vec{\alpha}|/\mu \sim 10^{-8}-10^{-7}$ . The ratios including  $\vec{\epsilon}$  or  $\vec{\alpha}$  are much smaller than those in the  $1 \hat{\nu}^c$  case. We find that 1-loop corrections to (44) are negligible if

$$\frac{|\vec{\alpha}|^2}{|\vec{\Lambda}|} \lesssim 10^{-3} \quad \text{and} \quad \frac{|\vec{\epsilon}|^2}{|\vec{\Lambda}|} \lesssim 10^{-3} \quad (50)$$

are fulfilled. Note that the mixing of the neutrinos with the higgsinos, given by the third column in the matrix  $\xi$  in Equation (39), depends not only on  $\alpha_i$  but also on  $\epsilon_i$ . This leads to 1-loop corrections to the neutrino mass matrix with pieces proportional to the  $\epsilon_i$  parameters, as it also happens in the  $1 \hat{\nu}^c$ -model. Therefore, both conditions in Equation (50) need to be fulfilled. Finally, in models with more generations of right-handed neutrinos there will be more freedom due to additional contributions to the neutrino mass matrix. For example, the case of three generations is discussed in [53], where the additional freedom is also used to generate an inverted hierarchy for the neutrino masses.

### III. CHOICE OF THE PARAMETERS AND EXPERIMENTAL CONSTRAINTS

In the subsequent sections we work out collider signatures for various scenarios. To facilitate the comparison with existing studies we adopt the following strategy: We take existing study points and augment them with the additional model parameters breaking R-parity. These points are SPS1a' [67], SPS3, SPS4, SPS9 [68] and the ATLAS SU4 point [69]. SPS1a' contains a relative light spectrum so that at LHC a high statistic can be achieved, SPS3 has a somewhat heavier spectrum and in addition the lightest neutralino and the lighter stau are close in mass which affects also the R-parity violating decays of the lightest neutralino. SPS4 is chosen because of the large  $\tan\beta$  value and SPS9 is an AMSB scenario where not only the lightest neutralino but also the lighter chargino has dominant R-parity violating decay modes. In all these points the lightest neutralino is so heavy that it can decay via two-body modes, as long as it's not a light  $\nu^c$ . In contrast for the SU4 point all two-body decay modes (at tree-level) are kinematically forbidden. As the parameters of these points are given at different scales we use the program **SPheno** [70] to evaluate them at  $Q = m_Z$  where we add the additional model parameters. Note that we allow  $\mu$  to depart from their standard SPS values to be consistent with the LEP bounds on Higgs masses, discussed below.

The additional model parameters are subject to theoretical and experimental constraints. In [52] the question of color and charge breaking minimas, perturbativity up to the GUT scale as well as the question of tachyonic states for the neutral scalar and pseudoscalars have been investigated. The last issue has already been addressed in Section IID where we derived conditions on the parameters. By choosing the coupling constants  $\lambda, \kappa < 0.6$  in the  $1 \hat{\nu}^c$ -model and  $\lambda_s, \kappa_s < 0.5$  in the  $2 \hat{\nu}^c$ -model, perturbativity up to the GUT scale is guaranteed [52]. Note, that choosing somewhat larger values for  $\lambda$  and/or  $\kappa$  up to 1 does not change any of the results presented below. We also address the question of color and charge breaking minimas by choosing  $\lambda_s > 0$ ,  $\kappa_s > 0$ ,  $T_\lambda^s > 0$ ,  $T_\kappa^{stu} < 0$ , whereas the Yukawa couplings  $h_\nu^{is}$  can either be positive or negative, but those values are small  $< \mathcal{O}(10^{-6})$  due to constraints from neutrino physics. Our  $T_{h_\nu}^{is}$  are negative, so the condition (2.8) of [52] is easy to fulfill.

Concerning experimental data we take the following constraints into account:

- We check that the neutrino data are fulfilled within the  $2\text{-}\sigma$  range given in Table I taken from ref. [12] if not stated otherwise. These data can easily be fitted using the effective neutrino mass matrices given in Section IIE.
- Breaking lepton number implies that flavour violating decays of the leptons like  $\mu \rightarrow e\gamma$  are possible, where strong experimental bounds exist [31]. However, in the model under study it turns out that these

parameter	best fit	2- $\sigma$
$\Delta m_{21}^2 [10^{-5} \text{eV}^2]$	$7.65_{-0.20}^{+0.23}$	$7.25 - 8.11$
$ \Delta m_{31}^2  [10^{-3} \text{eV}^2]$	$2.40_{-0.11}^{+0.12}$	$2.18 - 2.64$
$\sin^2 \theta_{12}$	$0.304_{-0.016}^{+0.022}$	$0.27 - 0.35$
$\sin^2 \theta_{23}$	$0.50_{-0.06}^{+0.07}$	$0.39 - 0.63$
$\sin^2 \theta_{13}$	$0.01_{-0.011}^{+0.016}$	$\leq 0.040$

Table I: Best-fit values with 1- $\sigma$  errors and 2- $\sigma$  intervals (1 d.o.f.) taken from [12]. In the following we will refer to these angles as  $\theta_{12} = \theta_{sol}$ ,  $\theta_{23} = \theta_{atm}$  and  $\theta_{13} = \theta_R$ .

bounds are automatically fulfilled once the constraints from neutrino physics are taken into account similar to the case of models with bilinear R-parity breaking [71].

- Bounds on the masses of the Higgs bosons [31, 72]. For this purpose we have added the dominant 1-loop correction to the (2,2) entry of the scalar mass matrix in Appendix A 2. Moreover, we have checked in the 1  $\hat{\nu}^c$ -model with the help of the program NMHDECAY [49] that in the NMSSM limit the experimental constraints are fulfilled.
- Constraints on the chargino and charged slepton masses given by the PDG [31].
- The bounds on squark and gluino masses from TEVATRON [31] are automatically fulfilled by our choices of the study points.

The smallness of the  $\hat{R}_p$  parameters guarantees that the direct production cross sections for the SUSY particles are very similar to the corresponding MSSM/NMSSM values. Note that for low values of  $\lambda$  the singlet states are decoupled from the rest of the particles, leading to low production rates.

#### IV. PHENOMENOLOGY OF THE 1 $\hat{\nu}^c$ -MODEL

In this section we discuss the phenomenology of the 1  $\hat{\nu}^c$ -model, including mass hierarchies, mixings in the scalar and fermionic sectors, decays of the scalar and fermionic states and the correlations between certain branching ratios and the neutrino mixing angles.

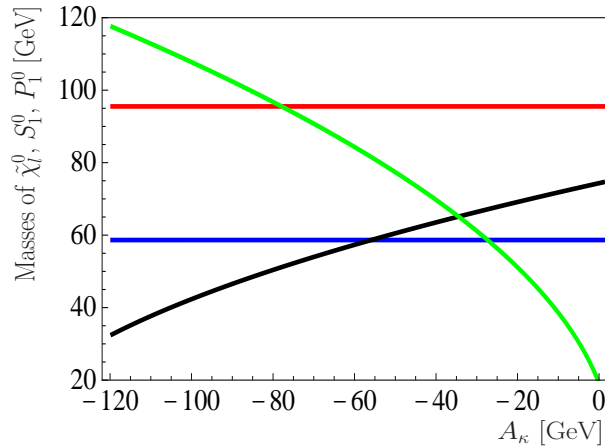


Figure 3: Masses of the lightest neutralinos  $\tilde{\chi}_l^0$  and the lightest scalar  $S_1^0 = Re(\tilde{\nu}^c)$ /pseudoscalar  $P_1^0 = Im(\tilde{\nu}_1^c)$  as a function of  $A_\kappa = T_\kappa/\kappa$  for  $\lambda = 0.24$ ,  $\kappa = 0.12$ ,  $\mu = 150\text{GeV}$  and  $T_\lambda = 360\text{GeV}$  for SPS1a'. The different colors refer to the singlino  $\tilde{\chi}_1^0$  (blue), the bino  $\tilde{\chi}_2^0$  (red), the singlet scalar  $S_1^0$  (black) and the singlet pseudoscalar  $P_1^0$  (green).

In the following discussion we call a neutralino  $\tilde{\chi}_l^0$  a bino (singlino) if  $|\mathcal{N}_{l+3,1}|^2 > 0.5$  ( $|\mathcal{N}_{l+3,5}|^2 > 0.5$ ). As discussed below, light scalar  $S_m^0$  or pseudoscalar states  $P_m^0$  appear, especially in case of the singlino being the lightest neutralino. In the following we discuss possible mass hierarchies and mixings in more detail.

The diagonal entry of the singlet right-handed neutrino in the mass matrix of the neutral fermions is  $M_R = \frac{1}{\sqrt{2}}\kappa v_R$ , see Appendix A 4. A singlino as lightest neutralino is obtained by choosing small values for  $\kappa$  and/or  $v_R$ . Since the masses of the four MSSM neutralinos are mainly fixed by the chosen SPS point, we can either generate a bino-like or a singlino-like lightest neutralino by varying  $\kappa$  and/or  $v_R$ , where the latter case means a variation of  $\lambda$  due to a fixed  $\mu$ -parameter. A light singlet scalar and/or pseudoscalar can be obtained by appropriate choices of  $T_\lambda$  and  $T_\kappa$ . An example spectrum is shown in Figure 3. The MSSM parameters have been chosen according to SPS1a' except for  $\mu = 150$  GeV. The scalar state  $S_2^0 = h^0$  can easily get too light to be consistent with current experimental data, although the production rate  $e^+e^- \rightarrow ZS_2^0$  is lowered, since a mixing with the lighter singlet scalar  $S_1^0 = \tilde{\nu}^c$  reduces its mass. By reducing  $\mu$  the mixing can be lowered (see mass matrices) and this problem can be solved.

Another example spectrum for neutral fermions is shown in Figure 4. Again SPS1a' parameters have been chosen, except  $\mu = 170$  GeV. As the figure demonstrates for this reduced value of  $\mu$  the states are usually quite mixed, which is important for their decay properties, as discussed below. Note that the abrupt change in composition in  $\tilde{\chi}_3^0$  is due to the level crossing in the mass eigenstates.

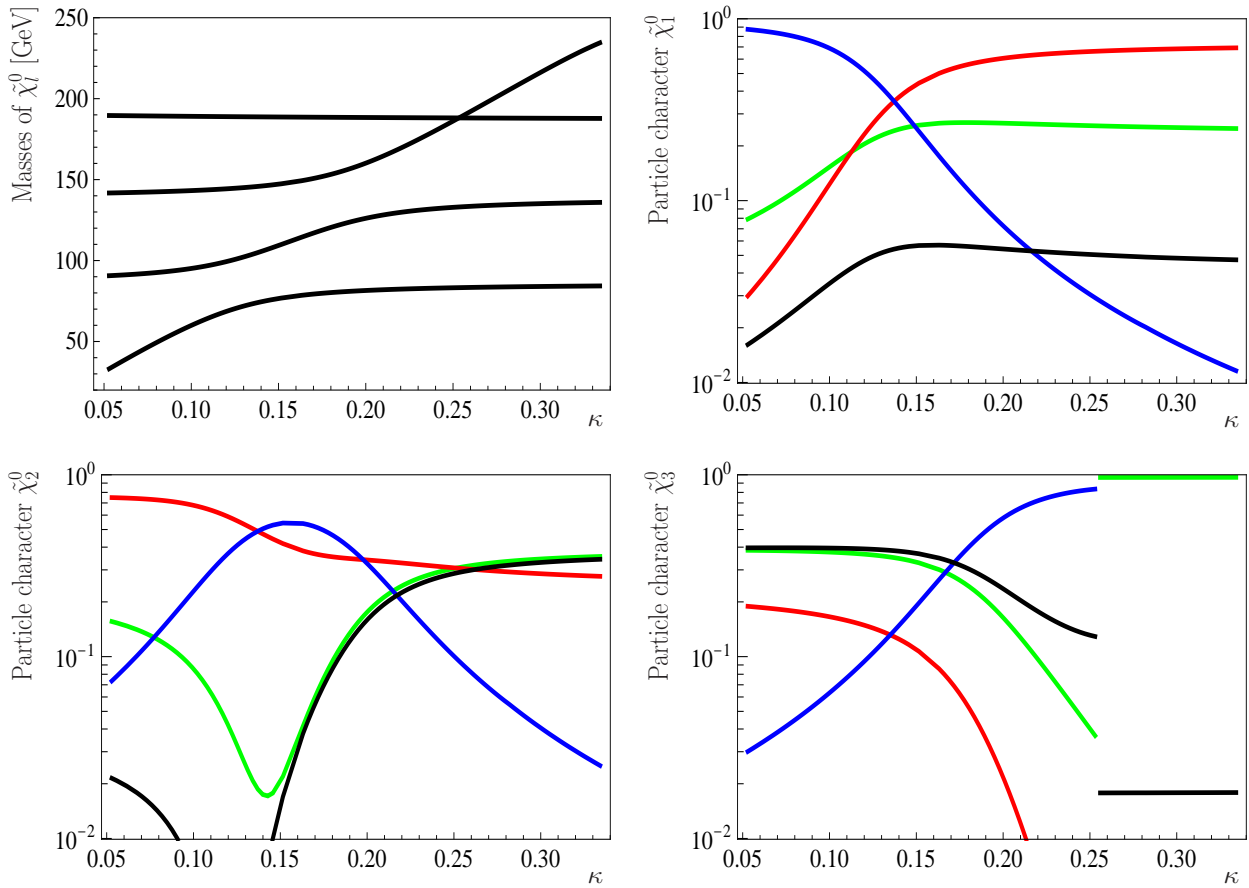


Figure 4: Masses and particle characters of the lightest neutralinos  $\tilde{\chi}_l^0$  as a function of  $\kappa$  for  $\lambda = 0.24$ ,  $\mu = 170$  GeV,  $T_\lambda = 360$  GeV and  $T_\kappa = -\kappa \cdot 50$  GeV for SPS1a'. The different colors refer to singlino purity  $|\mathcal{N}_{l+3,5}|^2$  (blue), bino purity  $|\mathcal{N}_{l+3,1}|^2$  (red), wino purity  $|\mathcal{N}_{l+3,2}|^2$  (black) and higgsino purity  $|\mathcal{N}_{l+3,3}|^2 + |\mathcal{N}_{l+3,4}|^2$  (green).

The decay properties of the lightest scalars/pseudoscalars are in general quite similar to those found in the NMSSM [50, 62]. The lightest doublet Higgs boson similar to the  $h^0$  decays mainly like in the MSSM, apart from the possible final state  $2\tilde{\chi}_1^0$ , if kinematically possible. An example is shown in Figure 5, which display the branching ratios of  $S_2^0 = h^0$  versus  $m(\tilde{\chi}_1^0)$ .  $\tilde{\chi}_1^0$  in this plot is mainly a singlino (see Figure 4), variation of  $\kappa$  varies its mass, since  $v_R$  is kept fixed here. In contrast to the NMSSM this does not lead to an invisible Higgs, since the neutralinos themselves decay. For the range of parameters where the decay to  $2\tilde{\chi}_1^0$  is large,  $\tilde{\chi}_1^0$  decays mainly to  $\nu b\bar{b}$ , leading to the final state 4  $b$ -jets plus missing energy. Note that the  $S_1^0$  which is mainly singlet here decays dominantly to  $b\bar{b}$  final states, followed by  $\tau\tau$  final states.

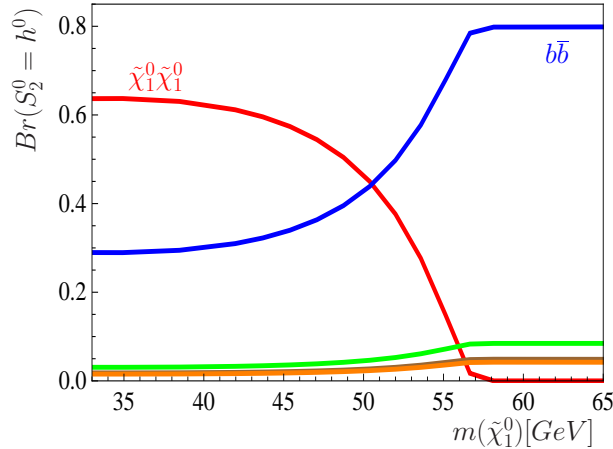


Figure 5: Branching ratios  $Br(S_2^0 = h^0)$  as a function of  $m(\tilde{\chi}_1^0)$  for the parameter set of Figure 4 (variation of  $\kappa$ ). The colors indicate the different final states:  $\tilde{\chi}_1^0\tilde{\chi}_1^0$  (red),  $b\bar{b}$  (blue),  $\tau^+\tau^-$  (green),  $c\bar{c}$  (orange) and  $Wq\bar{q}$  (brown).

### A. Decays of a gaugino-like lightest neutralino

We first consider the case of a bino as lightest neutralino. Although  $m(\tilde{\chi}_1^0) > m_W$  in the SPS points we have chosen, two-body decay modes are not necessarily dominant. The three-body decay  $\tilde{\chi}_1^0 \rightarrow l_i l_j \nu$  dominated by a virtual  $\tilde{\tau}$  also can have a sizeable branching ratio, see Table II and Figure 7. The importance of this final state can be understood from the Feynman graph shown in Figure 6, giving the dominant contribution due to  $\tilde{H}_d^-$ - $l_i$ -mixing ( $l_i = e, \mu$ ).

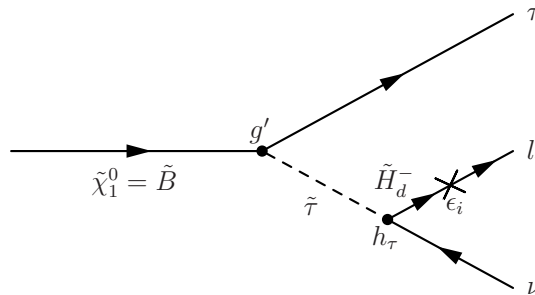


Figure 6: Dominant Feynman graph for the decay  $\tilde{\chi}_1^0 \rightarrow l_i \tau \nu$  with  $l_i = e, \mu$ .

In the case  $l_i = \tau$  there's an additional contribution due to  $\tilde{H}_d^0$ - $\nu$ -mixing. As Figure 7 shows there exist parameter combinations in the  $\lambda$ - $\kappa$ -plane, where the decay mode  $\tilde{\chi}_1^0 \rightarrow l_i l_j \nu$  is more important than

$\tilde{\chi}_1^0 \rightarrow Wl$ . The strong variation in the branching ratios for SPS1a' is mainly due to the strong dependence of the partial decay width of  $\tilde{\chi}_1^0 \rightarrow l_i l_j \nu$ , where the decays with  $i = j$  and  $i \neq j$  both play a role. Other important final states are  $\tilde{\chi}_1^0 \rightarrow Z\nu$  and in case of a light scalar with  $m(\tilde{\chi}_1^0) > m(h^0)$  the decay  $\tilde{\chi}_1^0 \rightarrow h^0 \nu$ , as demonstrated in Table II.

$Br(\tilde{\chi}_1^0)$	SPS1a'	SPS3	SPS4
$Wl$	23 – 80	12 – 55	68 – 72
$l_i l_j \nu$	11 – 75	2 – 31	2.6 – 3.9
$Z\nu$	2.2 – 8.9	5 – 28	25 – 28
$h^0 \nu$	–	15 – 53	< 2.0
Decay length [mm]	1.6 – 7.0	0.1 – 0.5	1.4 – 1.6

Table II: Branching ratios (in %) and total decay length in mm of the decay of the lightest bino-like neutralino for different values of  $\lambda \in [0.02, 0.5]$  and  $\kappa \in [0.1, 0.6]$  with a dependence of allowed  $\kappa(\lambda)$  similar to [52] and to Figure 7 and  $T_\lambda = \lambda \cdot 1.5\text{TeV}$  and  $T_\kappa = -\kappa \cdot 100\text{GeV}$ .

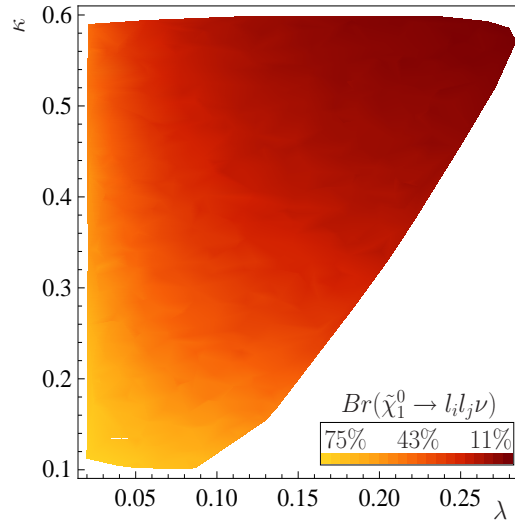


Figure 7: Dependence of allowed  $\kappa(\lambda)$  for values of  $\lambda \in [0.02, 0.5]$  and  $\kappa \in [0.1, 0.6]$  and  $Br(\tilde{\chi}_1^0 \rightarrow l_i l_j \nu)$  as function of  $\lambda$  and  $\kappa$  exemplary for SPS1a' with  $\mu = 390\text{GeV}$ ,  $T_\lambda = \lambda \cdot 1.5\text{TeV}$  and  $T_\kappa = -\kappa \cdot 100\text{GeV}$ .

In the  $\mu\nu\text{SSM}$  one finds correlation between the decays of the lightest neutralino and the neutrino mixing angles, because neutralino couplings depend on the same  $R_p$  parameters as the neutrino masses. Figure 8 shows the correlation between the branching ratios of the decay  $\tilde{\chi}_1^0 \rightarrow Wl$  as a function of the atmospheric angle. Although a clear correlation is visible it is not as pronounced as in the  $n$  generation case, see below and [53], due to inclusion of 1-loop effects in the neutrino masses and mixing angles.

Also the three-body decay  $\tilde{\chi}_1^0 \rightarrow l_i l_j \nu$  exemplifies a correlation with neutrino physics. However, this decay is connected to the solar angle, see Figure 9. There are two main contributions to this final state:  $\tilde{\chi}_1^0 \rightarrow Wl \rightarrow l_i l_j \nu$  and  $\tilde{\chi}_1^0 \rightarrow \tilde{\tau}^* l \rightarrow l_i l_j \nu$ . While the former is mainly sensitive to  $\Lambda_i$ , the latter is dominated by  $\epsilon_i$ -type couplings (see Figure 6), causing the connection to solar neutrino angle. In case the  $W$  is on-shell as in the SPS1a' point, one could in principle devise kinematical cuts reducing this contribution. Such a cut can significantly improve the quality of the correlation.

The SU4 scenario of the ATLAS collaboration [69] has a very light SUSY spectrum close to the Tevatron bound with a bino-like neutralino  $m(\tilde{\chi}_1^0) \approx 60\text{ GeV}$ . Thus, for SU4 the lightest neutralino has only three-body decay modes. Most important branching ratios are shown in Figure 10. The lightness of the bino-like

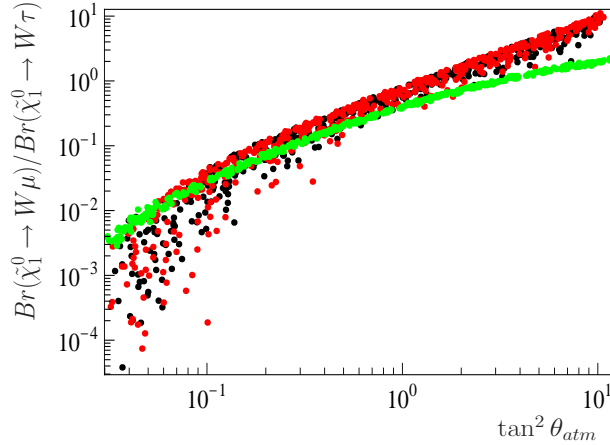


Figure 8: Ratio  $\frac{Br(\tilde{\chi}_1^0 \to W\mu)}{Br(\tilde{\chi}_1^0 \to W\tau)}$  versus  $\tan^2 \theta_{atm}$  for different SPS scenarios (SPS1a' (black), SPS3 (red), SPS4 (green)) and for different values of  $\lambda \in [0.02, 0.5]$  and  $\kappa \in [0.1, 0.6]$  with a dependence of allowed  $\kappa(\lambda)$  similar to [52] and to Figure 7 and  $T_\lambda = \lambda \cdot 1.5\text{TeV}$  and  $T_\kappa = -\kappa \cdot 100\text{GeV}$ .

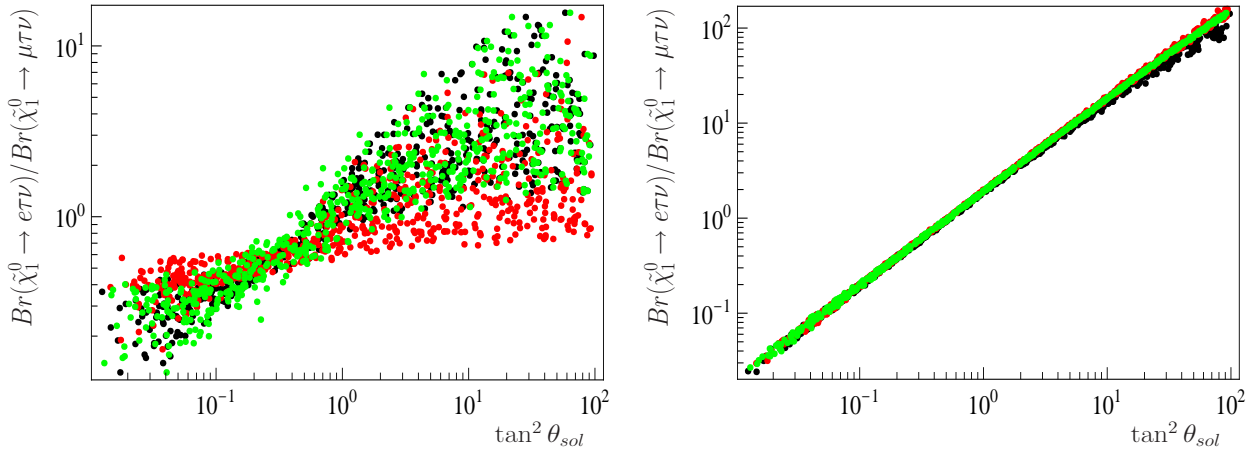


Figure 9: Ratio  $\frac{Br(\tilde{\chi}_1^0 \to e\tau\nu)}{Br(\tilde{\chi}_1^0 \to \mu\tau\nu)}$  versus  $\tan^2 \theta_{sol}$  with same set of parameters as Figure 8. Bino purity  $|\mathcal{N}_{41}|^2 > 0.97$ . To the left (a) two-body plus three-body contributions, to the right (b) three-body contributions only. For a discussion see text.

neutralino  $\tilde{\chi}_1^0$  in this scenario implies a larger average decay length of (8–90) cm, depending on the parameter point in the  $\lambda$ - $\kappa$ -plane. Note that the decay length becomes smaller for smaller values of  $\lambda, \kappa$ . In general the decay length scales as  $L \propto m^{-4}(\tilde{\chi}_1^0)$  for  $m(\tilde{\chi}_1^0) < m_W$ . Also for this point a correlation between the branching ratios and the neutrino mixing angles is found as illustrated in Figure 11.

In addition to the SUGRA scenarios discussed up to now we have also studied SPS9, which is a typical AMSB point. The most important difference between this point and the previously discussed cases is the near degeneracy between lightest neutralino and lightest chargino. This near degeneracy is the reason that the chargino decay is dominated by  $\tilde{R}_p$  final states. Varying  $\lambda$  and  $\kappa$  as before we find a total decay length of (0.12 – 0.16)mm with  $Br(\tilde{\chi}_1^\pm \to W\nu) = (42 - 57)\%$ ,  $Br(\tilde{\chi}_1^\pm \to Zl) = (20 - 26)\%$  and  $Br(\tilde{\chi}_1^\pm \to h^0 l) = (17 - 40)\%$ . This is especially interesting since, similar to  $Wl$  in case of the gaugino-like lightest neutralino, the decay to  $Zl$  of the chargino is linked to the atmospheric angle, see Figure 12.



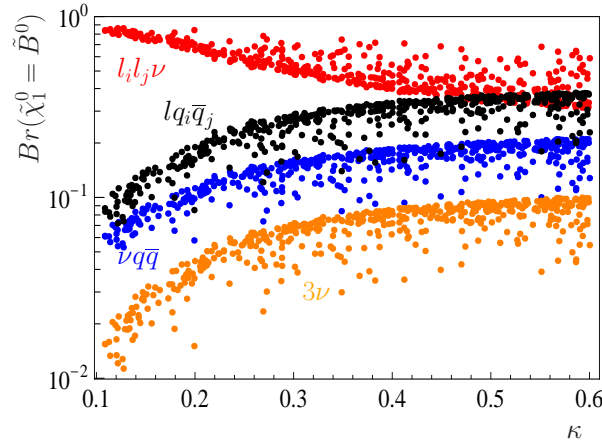


Figure 10: Decay branching ratios for bino-like lightest neutralino as a function of  $\kappa$  for  $\lambda \in [0.02, 0.5]$ ,  $T_\lambda = \lambda \cdot 1.5$  TeV,  $T_\kappa = -\kappa \cdot 100$  GeV and for MSSM parameters defined by the study point SU4 of the ATLAS collaboration [69]. The colors indicate the different final states:  $l_i l_j \nu$  (red),  $l q_i \bar{q}_j$  (black),  $\nu q \bar{q}$  (blue) and  $3\nu$  (orange).

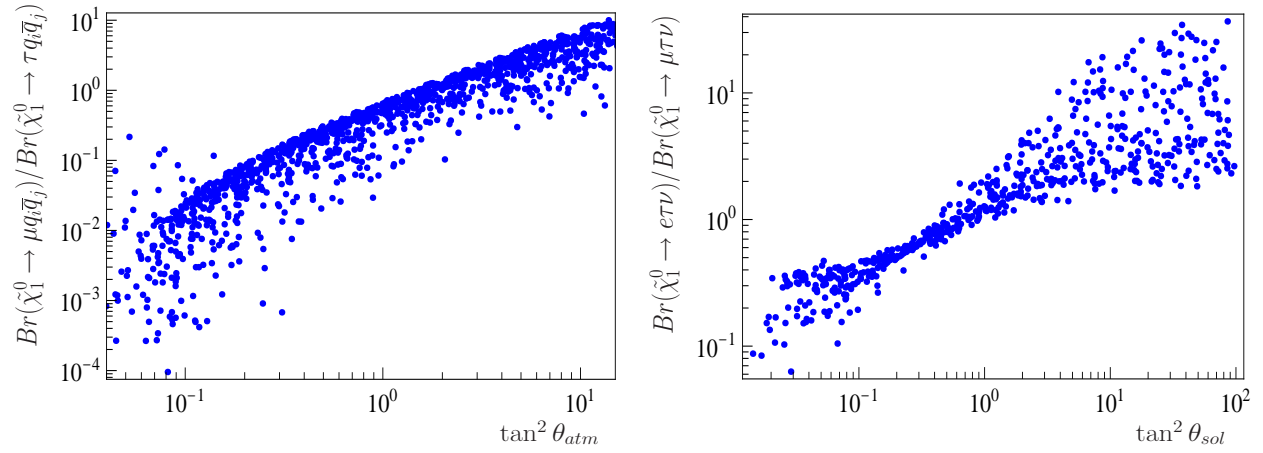


Figure 11: To the left (a) ratio  $\frac{Br(\tilde{\chi}_1^0 \rightarrow \mu q_i \bar{q}_j)}{Br(\tilde{\chi}_1^0 \rightarrow \tau q_i \bar{q}_j)}$  versus  $\tan^2 \theta_{atm}$  for the SU4 scenario of the ATLAS collaboration [69] and to the right (b) ratio  $\frac{Br(\tilde{\chi}_1^0 \rightarrow e\tau\nu)}{Br(\tilde{\chi}_1^0 \rightarrow \mu\tau\nu)}$  versus  $\tan^2 \theta_{sol}$  with same set of parameters as (a). Bino purity  $|\mathcal{N}_{41}|^2 > 0.94$ .

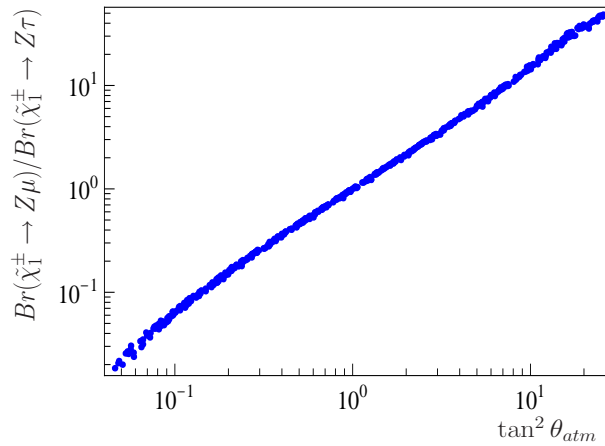


Figure 12: Ratio  $\frac{Br(\tilde{\chi}_1^\pm \rightarrow Z\mu)}{Br(\tilde{\chi}_1^\pm \rightarrow Z\tau)}$  versus  $\tan^2 \theta_{atm}$  for the AMSB scenario SPS9 and for different values of  $\lambda \in [0.02, 0.5]$ ,  $\kappa \in [0.1, 0.6]$ ,  $T_\lambda = \lambda \cdot 1.5$  TeV and  $T_\kappa = -\kappa \cdot 100$  GeV.

## B. Decays of a singlino-like lightest neutralino

We now turn to the case of a singlino-like LSP. As already explained, this scenario is connected to a light singlet scalar and pseudoscalar. Recall, that the particles in the fermionic sector are mixed for  $\lambda, \kappa = \mathcal{O}(10^{-1})$  due to the reduced  $\mu$ -parameter as can be seen in Figure 4. We will first discuss the average decay length of the lightest neutralino  $\tilde{\chi}_1^0$ . Figure 13 shows the average decay length in meter for different SPS scenarios as a function of the mass of the lightest neutralino  $m(\tilde{\chi}_1^0)$ . Composition of the neutralino is indicated by colour code, as given in the caption.  $\lambda, \kappa, T_\kappa$  and  $\mu$  are varied in this plot. Note that by variation of  $T_\kappa$  the parameter points in Figure 13 are chosen in such a way, that all scalar and pseudoscalar states are heavier than the lightest neutralino. Singlino purity in this plot increases with decreasing mass and for pure singlinos the decay length is mainly determined by its mass and the experimentally determined neutrino masses. For neutralino masses below about 50 GeV decay lengths become larger than 1 meter, implying that a large fraction of neutralinos will decay outside typical collider detectors. Note that if one allows for lighter scalar states so that at least one of the decays  $\tilde{\chi}_1^0 \rightarrow S_1^0(P_1^0)\nu$  appears, the average decay length can be easily reduced by several orders of magnitude.

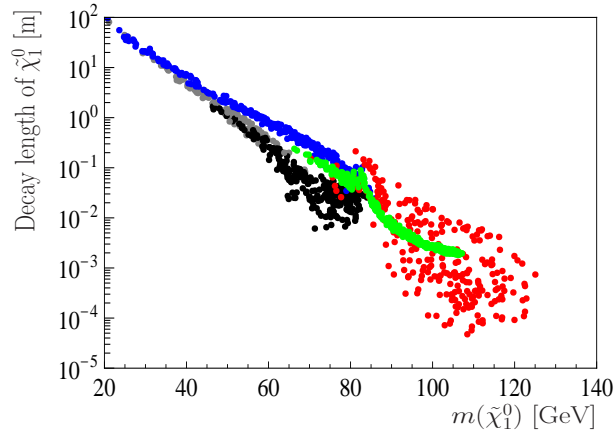


Figure 13: Decay length of the lightest neutralino  $\tilde{\chi}_1^0$  in m as a function of its mass  $m(\tilde{\chi}_1^0)$  in GeV for different values of  $\lambda \in [0.2, 0.5]$ ,  $\kappa \in [0.025, 0.2]$  and  $\mu \in [110, 170]$  GeV with a dependence of allowed  $\kappa(\lambda)$  similar to [52] and to Figure 7 and  $T_\lambda = \lambda \cdot 1.5$  TeV, whereas  $T_\kappa \in [-20, -0.05]$  GeV is chosen in such a way, that no lighter scalar or pseudoscalar states with  $\{m(S_1^0), m(P_1^0)\} < m(\tilde{\chi}_1^0)$  appear. Note that the different colors stand for SPS1a' (real singlino,  $|\mathcal{N}_{45}|^2 > 0.5$ ) (gray), SPS1a' (mixture state) (black), SPS3 (real singlino) (blue), SPS3 (mixture state) (red) and SPS4 (mixture state) (green).

Again typical decays are  $Wl, lq_i\bar{q}_j, Z\nu, \nu q\bar{q}, l_i l_j \nu$  and the invisible decay to  $3\nu$ . For the region of  $m(\tilde{\chi}_1^0)$  below the  $W$  threshold see Figure 14. The dominance of  $\nu b\bar{b}$  for smaller values of  $m(\tilde{\chi}_1^0)$  is due to the decay chain  $\tilde{\chi}_1^0 \rightarrow S_1^0 \nu \rightarrow \nu b\bar{b}$ , whereas for larger values of  $m(\tilde{\chi}_1^0)$  we find  $m(S_1^0) > m(\tilde{\chi}_1^0)$ . Final state ratios show correlations with neutrino physics also in this case. As an example we show  $l_i l_j \nu$  branching ratios versus the solar neutrino mixing angle in Figure 15. Singlino purity for this plot  $|\mathcal{N}_{45}|^2 \in [0.75, 0.83]$  and mass  $m(\tilde{\chi}_1^0) \in [22, 53]$  GeV. The absolute values for the branching ratios are comparable to those of the described SU4 scenario with a bino-like lightest neutralino. We note that for the parameters in Figure 15 the light Higgs  $S_2^0 = h^0$  decays to  $\tilde{\chi}_1^0 \tilde{\chi}_1^0$  with a branching ratio of  $Br(S_2^0 = h^0 \rightarrow \tilde{\chi}_1^0 \tilde{\chi}_1^0) = (21 - 91)\%$ .

Up to now we have considered values of  $\lambda$  and  $\kappa$  larger than  $10^{-2}$ . For very small values of these couplings, the singlet sector, although very light, effectively decouples. This implies that R-parity conserving decays of  $\tilde{\chi}_2^0$ , e.g. decays to final states like  $\tilde{\chi}_1^0 S_1^0, \tilde{\chi}_1^0 P_1^0, \tilde{\chi}_1^0 l^+ l^-$  or  $\tilde{\chi}_1^0 q\bar{q}$ , are strongly suppressed and the  $\tilde{R}_p$  decay modes dominate, implying decays with correlations as in the case of the explicit b- $\tilde{R}_p$ .

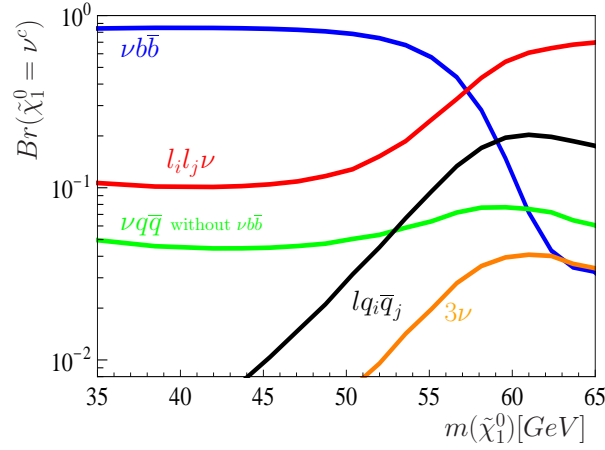


Figure 14: Singlino decay branching ratios as a function of its mass, for the same parameter choices as in Figure 5. The colors indicate the different final states:  $\nu b\bar{b}$  (blue),  $l_i l_j \nu$  (red),  $l q_i \bar{q}_j$  (black),  $3\nu$  (orange) and  $\nu q\bar{q}$  ( $q \neq b$ , green).

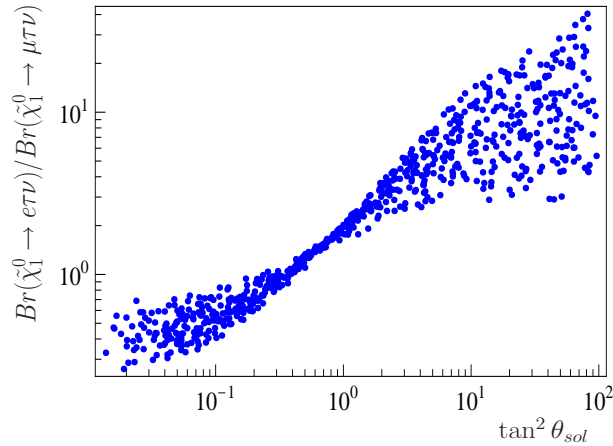


Figure 15: Ratio  $\frac{Br(\tilde{\chi}_1^0 \rightarrow e\tau\nu)}{Br(\tilde{\chi}_1^0 \rightarrow \mu\tau\nu)}$  versus  $\tan^2 \theta_{sol}$  for the SPS1a' scenario and  $\lambda \in [0.2, 0.5]$ ,  $\mu \in [110, 170]$  GeV,  $\kappa = 0.035$ ,  $T_\lambda = \lambda \cdot 1.5$  TeV and  $T_\kappa = -0.7$  GeV.

## V. PHENOMENOLOGY OF THE $n$ $\hat{\nu}^c$ -MODEL

In the previous section the phenomenology for the one generation case of the model has been worked out in detail. Most of the signals discussed so far are independent of the number of right-handed neutrinos. However, the  $n$  generation variants also offer some additional phenomenology, which we discuss here for the simplified case of  $n = 2$ .

In a model with one right-handed neutrino superfield a light singlino will always imply a light scalar/pseudoscalar. This connection between the neutral fermion sector and scalar/pseudoscalar sector is a well-known property of the NMSSM (see again [61, 62]). In models with more than one generation of singlets, the off-diagonal  $T_\kappa$  terms in Equation (5) induce mixing between the different generations of singlet scalars and pseudoscalars. This opens up the possibility, not considered in previous publications [51, 52, 53], to have the singlet scalars considerably heavier than the singlet fermions.

Let us illustrate this feature with a simple example. Imagine a light singlino  $\nu_1^c$ , and a heavy singlino  $\nu_2^c$ , in a model with non-zero trilinear couplings  $T_\kappa^{112}$ . In that case, the contributions to the mass of the  $\tilde{\nu}_1^c$ , scalar or pseudoscalar, coming from the large value of  $v_{R2}$  are proportional to  $T_\kappa^{112}$ . Without these

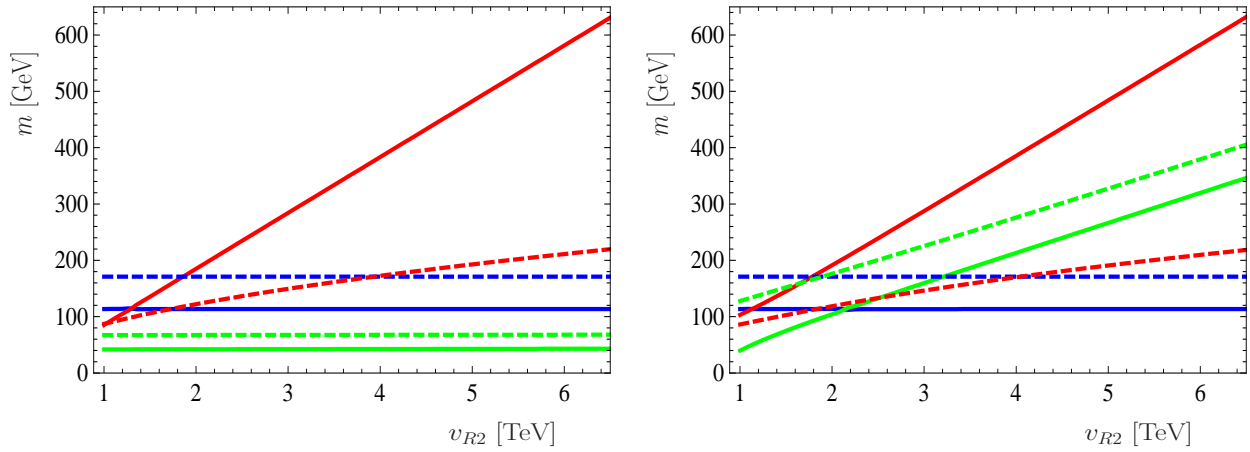


Figure 16: Masses of the scalar states  $Re(\tilde{\nu}_1^c)$  (green),  $Re(\tilde{\nu}_2^c)$  (red) and  $h^0$  (blue) and the pseudoscalar states  $Im(\tilde{\nu}_1^c)$  (dashed green),  $Im(\tilde{\nu}_2^c)$  (dashed red) and  $Im(\tilde{\nu}_1)$  (dashed blue) as a function of  $v_{R2}$  for different values of  $T_{\kappa}^{112} = T_{\kappa}^{122}$ . To the left (a)  $T_{\kappa}^{112} = T_{\kappa}^{122} = 0$  whereas to the right (b)  $T_{\kappa}^{112} = T_{\kappa}^{122} = -2$  GeV. The MSSM parameters have been taken such that the standard SPS1a' point is reproduced. The light singlet parameters  $\kappa_1 = 0.16$  and  $v_{R1} = 500$  GeV ensure that in all points the lightest neutralino is mostly  $\nu_1^c$ , with a mass of  $47 - 48$  GeV. In addition,  $T_{\lambda}^1 = 300$  GeV and  $T_{\lambda}^2 \in [10, 200]$  GeV.

contributions the mass of  $\tilde{\nu}_1^c$  would only depend on the small  $v_{R1}$ , thus making it light like the singlino of the same generation. With non-zero  $T_{\kappa}^{112}$  the mass of both  $\tilde{\nu}_s^c$  are dominated by the larger of the  $v_{Rs}$ . This feature is demonstrated in Figure 16. In the two plots the lightest neutralino is mostly  $\nu_1^c$ , with a mass of  $\sim 50$  GeV. These plots show the dependence of the masses of the singlet scalar states  $Re(\tilde{\nu}_1^c)$  and  $Re(\tilde{\nu}_2^c)$  and the corresponding pseudoscalar states  $Im(\tilde{\nu}_1^c)$  and  $Im(\tilde{\nu}_2^c)$  with  $v_{R2}$  for different values of  $T_{\kappa}^{112} = T_{\kappa}^{122}$ . The masses of the light Higgs boson  $h^0$  and the lightest left-handed sneutrino  $Im(\tilde{\nu}_1)$  are also shown for reference. Note that for  $T_{\kappa}^{112} = T_{\kappa}^{122} = 0$  the mass of the state  $Re(\tilde{\nu}_1^c)$  does not depend on  $v_{R2}$ , whereas for  $T_{\kappa}^{112} = T_{\kappa}^{122} = -2$  GeV the lightest singlet scalar becomes heavier for larger values of  $v_{R2}$ . The same feature is present in the pseudoscalar sector, where the effect is even more pronounced.

### A. Correlations with neutrino mixing angles in the $n \hat{\nu}^c$ -model

The connection between decays and neutrino angles is not a particular property of the  $1 \hat{\nu}^c$ -model and is also present in a general  $n \hat{\nu}^c$ -model. However, since the structure of the approximate couplings  $\tilde{\chi}_1^0 - W^{\pm} - l_i^{\mp}$  is different, see Appendix B, we encounter additional features for  $n = 2$ .

As explained in Section IIE2, we have now two possibilities to fit neutrino data. If the dominant contribution to the neutrino mass matrix comes from the  $\Lambda_i \Lambda_j$  term in Equation (44) one can link it to the atmospheric mass scale, using the  $\alpha_i \alpha_j$  term to fit the solar mass scale. This case will be called option fit1. On the other hand, if the dominant contribution is given by the  $\alpha_i \alpha_j$  term one has the opposite situation, where the atmospheric scale is fitted by the  $\alpha_i$  parameters and the solar scale is fitted by the  $\Lambda_i$  parameters. This case will be called option fit2.

For the case of a bino-like lightest neutralino one can show that the coupling is proportional to  $\Lambda_i$  whereas for the case of a singlino-like lightest neutralino the dependence is on  $\alpha_i$ , as shown in Appendix B. Figure 17 shows the ratio  $Br(\tilde{\chi}_1^0 \rightarrow W\mu)/Br(\tilde{\chi}_1^0 \rightarrow W\tau)$  versus  $\tan^2(\theta_{atm})$  (left) and  $Br(\tilde{\chi}_1^0 \rightarrow We)/\sqrt{Br(\tilde{\chi}_1^0 \rightarrow W\mu)^2 + Br(\tilde{\chi}_1^0 \rightarrow W\tau)^2}$  versus  $\sin^2(\theta_R)$  (right) for a bino LSP and option fit1. The correlation with the atmospheric angle and the upper bound on  $Br(\tilde{\chi}_1^0 \rightarrow We)/\sqrt{Br(\tilde{\chi}_1^0 \rightarrow W\mu)^2 + Br(\tilde{\chi}_1^0 \rightarrow W\tau)^2}$  from  $\sin^2(\theta_R)$  is more pronounced than in the  $1 \hat{\nu}^c$ -model, because we fit neutrino data with tree-level physics only. Recall that this implies that the ratio  $|\tilde{e}|^2/|\tilde{\Lambda}|$  is much smaller than in the plots shown in the previous section. A correlation between  $Br(\tilde{\chi}_1^0 \rightarrow We)/\sqrt{Br(\tilde{\chi}_1^0 \rightarrow W\mu)^2 + Br(\tilde{\chi}_1^0 \rightarrow W\tau)^2}$  and  $\tan^2(\theta_{sol})$  is found instead, if neutrino data is fitted with option fit2, as Figure 18 shows.

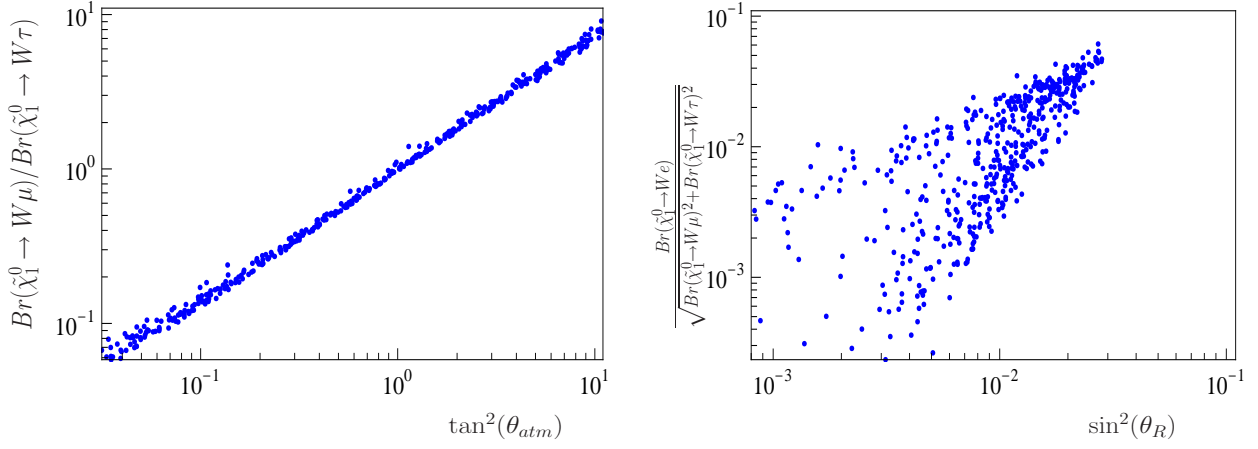


Figure 17: To the left (a) ratio  $\frac{Br(\tilde{\chi}_1^0 \rightarrow W\mu)}{Br(\tilde{\chi}_1^0 \rightarrow W\tau)}$  versus  $\tan^2(\theta_{atm})$  and to the right (b) ratio  $\frac{Br(\tilde{\chi}_1^0 \rightarrow W e)}{\sqrt{Br(\tilde{\chi}_1^0 \rightarrow W\mu)^2 + Br(\tilde{\chi}_1^0 \rightarrow W\tau)^2}}$  versus  $\sin^2(\theta_R)$  for a bino LSP. Bino purity  $|\mathcal{N}_{41}|^2 > 0.9$ . Neutrino data is fitted using option fit1.

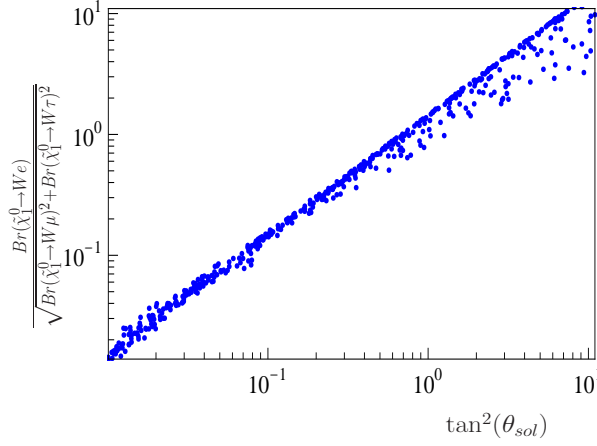


Figure 18: Ratio  $\frac{Br(\tilde{\chi}_1^0 \rightarrow W e)}{\sqrt{Br(\tilde{\chi}_1^0 \rightarrow W\mu)^2 + Br(\tilde{\chi}_1^0 \rightarrow W\tau)^2}}$  versus  $\tan^2(\theta_{sol})$  for a bino LSP. Bino purity  $|\mathcal{N}_{41}|^2 > 0.9$ . Neutrino data is fitted using option fit2.

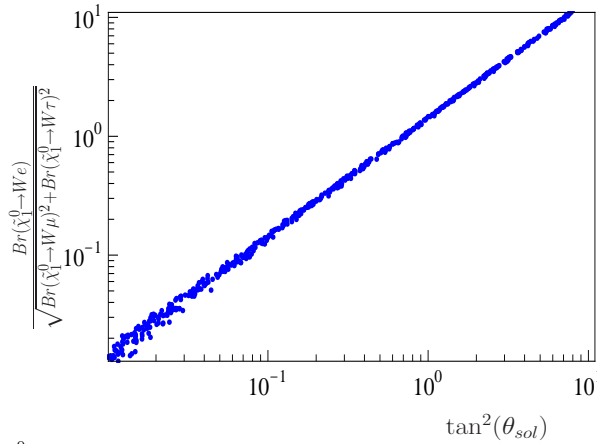


Figure 19: Ratio  $\frac{Br(\tilde{\chi}_1^0 \rightarrow W e)}{\sqrt{Br(\tilde{\chi}_1^0 \rightarrow W\mu)^2 + Br(\tilde{\chi}_1^0 \rightarrow W\tau)^2}}$  versus  $\tan^2(\theta_{sol})$  for a singlino LSP. Singlino purity  $|\mathcal{N}_{45}|^2 > 0.9$ . Neutrino data is fitted using option fit1.

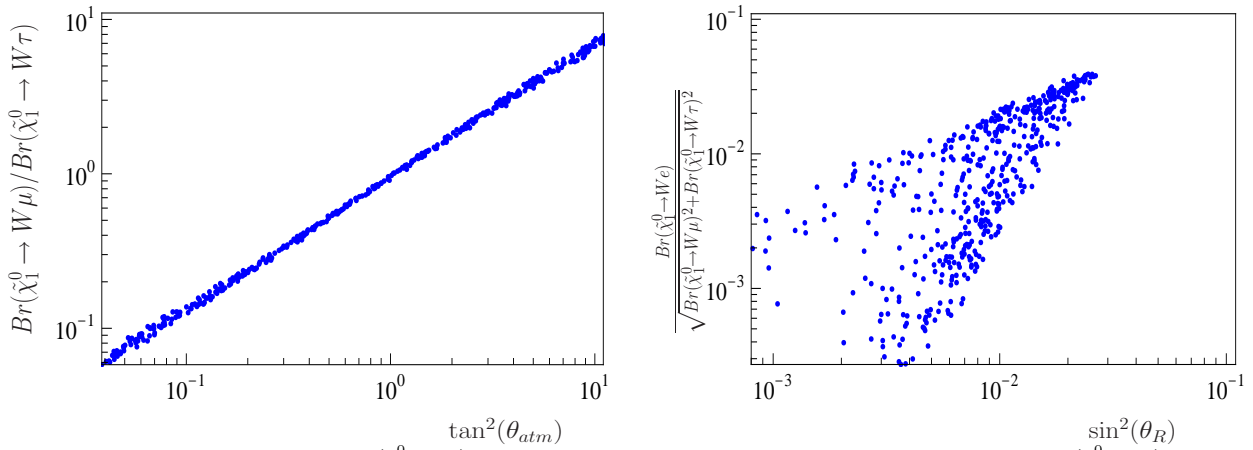


Figure 20: To the left (a) ratio  $\frac{Br(\tilde{\chi}_1^0 \rightarrow W\mu)}{Br(\tilde{\chi}_1^0 \rightarrow W\tau)}$  versus  $\tan^2(\theta_{atm})$  and to the right (b) ratio  $\frac{Br(\tilde{\chi}_1^0 \rightarrow We)}{\sqrt{Br(\tilde{\chi}_1^0 \rightarrow W\mu)^2 + Br(\tilde{\chi}_1^0 \rightarrow W\tau)^2}}$  versus  $\sin^2(\theta_R)$  for a singlino LSP. Singlino purity  $|\mathcal{N}_{45}|^2 > 0.9$ . Neutrino data is fitted using option fit2.

For the case of a singlino LSP the correlations and types of fit to neutrino data are swapped with respect to the gaugino case. Since the couplings  $\tilde{\chi}_1^0 - W^\pm - l_i^\mp$  are mainly proportional to  $\alpha_i$ , instead of  $\Lambda_i$ , a scenario with a singlino LSP and option fit1 (fit2) will be similar to bino LSP and option fit2 (fit1). This similarity is demonstrated in Figures 19 and 20. To decide which case is realized in nature, one would need to determine the particle character of the lightest neutralino. This might be difficult at the LHC, but could be determined by a cross section measurement at the ILC. We want to note, that in the 2  $\hat{\nu}^c$ -model we cannot reproduce all correlations for a singlino LSP presented for the 3  $\hat{\nu}^c$ -model in [53].

The results shown so far in this section were all calculated for the SPS1a' scenario. We have checked explicitly that for all the other standard points results remain unchanged. We have also checked that for a LSP with a mass below  $m_W$  the three-body decays  $\tilde{\chi}_1^0 \rightarrow lq_i \bar{q}_j$ , mediated by virtual  $W$  bosons, show the same correlations.

A final comment is in order. In a  $n$   $\hat{\nu}^c$ -model with  $n > 2$ , the effective neutrino mass matrix will have additional terms with respect to (44), due to the contributions coming from the new right-handed neutrinos. For this richer structure there is one additional contribution to  $\mathbf{m}_{\nu\nu}^{\text{eff}}$ , which could be subdominant. Therefore, one can imagine a scenario in which a third generation of singlets produces a negligible contribution to neutrino masses while the corresponding singlino,  $\nu_3^c$ , is the LSP. In such a scenario the correlations between the  $\nu_3^c$  LSP decays and the neutrino mixing angles will be lost.

### B. $\tilde{\chi}_1^0$ decay length and type of fit

As already discussed we have two different possibilities to fit neutrino data:  $\vec{\Lambda}$  generates the atmospheric mass scale and  $\vec{\alpha}$  the solar mass scale (case fit1), or vice versa (case fit2). It turns out that the decay length of the lightest neutralino is sensitive to the type of fit, due to the proportionality between its couplings with gauge bosons and the  $\vec{R}_p$  parameters (see Appendix B for exact and approximated formulas of the couplings  $\tilde{\chi}_1^0 - W^\pm - l_i^\mp$  and their simplified expressions in particular limits). For example, a singlino-like neutralino couples to the gauge bosons proportionally to the  $\alpha_i$  parameters. This implies that its decay length will follow  $L \propto 1/|\vec{\alpha}|^2$  and obeys the approximate relation

$$\frac{L(\text{fit1})}{L(\text{fit2})} \simeq \frac{m_{atm}}{m_{sol}} \simeq 6 \quad . \quad (51)$$

In Figure 21 the decay length of the lightest neutralino and its dependence on the type of fit to neutrino data is shown. Once mass and length are known this dependence can be used to determine which parameters generate which mass scale. Note that this feature is essentially independent of the MSSM parameters.

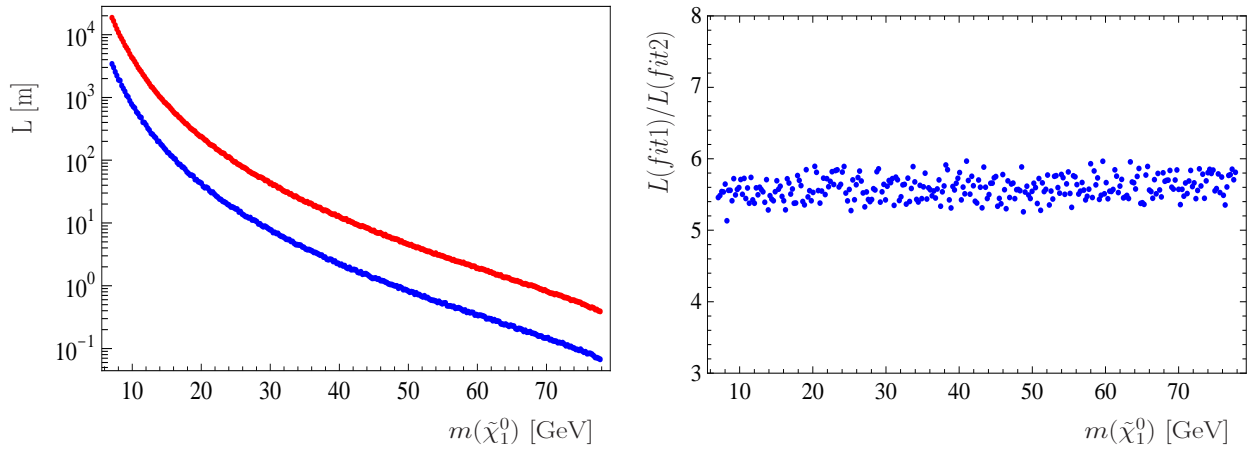


Figure 21: Decay length of the lightest neutralino and its dependence on the type of fit to neutrino data. To the left (a) the decay length of the lightest neutralino versus  $m(\tilde{\chi}_1^0)$  for the case fit1 (red) and the case fit2 (blue). To the right (b) the ratio  $L(\text{fit1})/L(\text{fit2})$  versus  $m(\tilde{\chi}_1^0)$ . The MSSM parameters have been taken such that the standard SPS1a' point is reproduced. The light singlet parameter  $\kappa$  is varied in the range  $\kappa \in [0.01, 0.1]$ . In all the points the lightest neutralino has a singlino purity higher than 0.99.

However, this property is lost if either the lightest neutralino has a sizeable gaugino/higgsino component or if there are singlet scalars/pseudoscalars lighter than the singlino.

### C. Several light singlets

In scenarios with two (or more) light singlets, the phenomenology has additional features. The light Higgs boson  $h^0$  can decay with measurable branching ratios to pairs of right-handed neutrinos of different generations. Similarly, the bino can decay to the different light right-handed neutrinos.

In the following, the case of two light singlinos and two light scalars/pseudoscalars will be considered. For the neutral fermion sector this implies that the mass eigenstates  $\tilde{\chi}_1^0$  and  $\tilde{\chi}_2^0$  will always be the singlets  $\nu_1^c$  and  $\nu_2^c$  and the bino will be the  $\tilde{\chi}_3^0$ . In the scalar sector one has two very light mostly singlet states  $S_1^0$  and  $S_2^0$ , which are consistent with the LEP bounds. Finally, the state  $S_3^0$  will be the light doublet Higgs boson  $h^0$ . One can also have light singlet pseudoscalars.

The decays of a bino-like  $\tilde{\chi}_3^0$  can be very important to distinguish between the one generation model and models with more than one generation of singlets. In principle, the most important decay channels strongly depend on the couplings of the bino to the two generations of singlinos and the configuration of masses of singlinos and scalars. Therefore, a general list of signals cannot be given. Nevertheless, there are some features which are always present:

When kinematically allowed, the decays  $\tilde{\chi}_3^0 \rightarrow \tilde{\chi}_{1,2}^0 S_1^0(P_1^0)$  dominate, with the sum of the branching ratios typically larger than 50%. The relative importance of the different channels is mainly dictated by kinematics. This feature is illustrated in Figure 22, where these two quantities are shown as a function of the mass of the lightest neutralino. The MSSM parameters are fixed to the standard point SPS1a', with light singlet parameters taken randomly. One can see that the relative importance of each singlino cannot be predicted in general, but both branching ratios are at least of order  $10^{-3} - 10^{-4}$ , given enough statistics. For very light singlinos two-body decays including scalars and pseudoscalars are open, and thus both  $Br(\tilde{\chi}_3^0 \rightarrow \tilde{\chi}_1^0)$  and  $Br(\tilde{\chi}_3^0 \rightarrow \tilde{\chi}_2^0)$  are close to 50%, as expected if the values of the singlet parameters are of the same order for the two light generations. On the other hand, if the mass of the lightest neutralino is increased some of the two-body decays are kinematically forbidden, specially those of the  $\tilde{\chi}_2^0$ , which has to be produced through three-body decays, leading to a suppression in  $Br(\tilde{\chi}_3^0 \rightarrow \tilde{\chi}_2^0)$ . Note that it is also possible to find points where the decay mode  $\tilde{\chi}_3^0 \rightarrow \tilde{\chi}_{1,2}^0 S_2^0(P_2^0)$  has a branching ratio about 10%-20%, giving additional information.

The other possible signals are the usual bino decays of the NMSSM. Final states with standard model

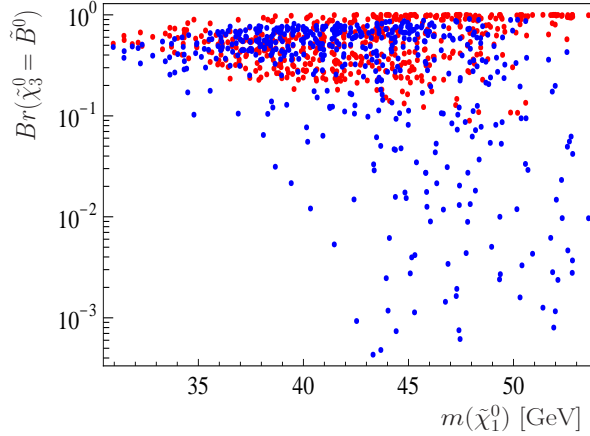


Figure 22: Branching ratios  $Br(\tilde{\chi}_3^0 = \tilde{B}^0 \rightarrow \tilde{\chi}_1^0)$  (red) and  $Br(\tilde{\chi}_3^0 = \tilde{B}^0 \rightarrow \tilde{\chi}_2^0)$  (blue) as a function of the mass of the lightest neutralino for the scenario considered in Section V C. The MSSM parameters have been taken such that the standard SPS1a' point is reproduced, whereas the singlet parameters are chosen randomly in the ranges  $v_{R1}, v_{R2} \in [400, 600]$  GeV,  $\lambda_1, \lambda_2 \in [0.0, 0.4]$ ,  $T_\kappa^{111} = T_\kappa^{222} \in [-15, -1]$  GeV,  $T_\kappa^{112} = T_\kappa^{122} \in [-1.5, -0.005]$  GeV and  $T_\lambda^1, T_\lambda^2 \in [0, 600]$  GeV.  $\kappa_1 = \kappa_2 = 0.16$  is fixed to ensure the lightness of the two singlinos.

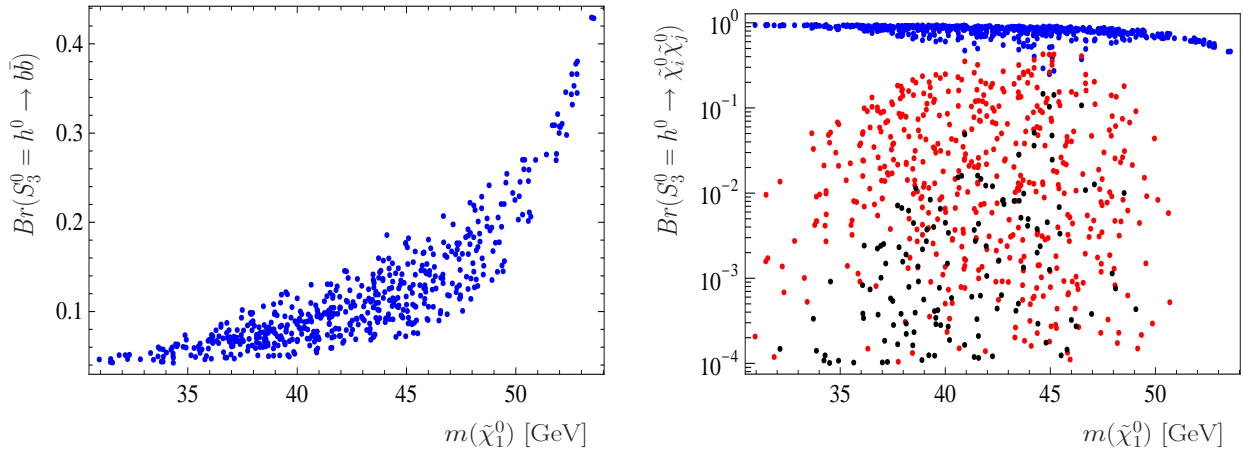


Figure 23: Higgs boson decays as a function of the mass of the lightest neutralino for the scenario considered in Section V C. To the left (a) the standard decay channel  $h^0 \rightarrow b\bar{b}$ , whereas to the right (b) the exotic decays to pairs of singlinos  $h^0 \rightarrow \tilde{\chi}_1^0 \tilde{\chi}_1^0$  (red),  $h^0 \rightarrow \tilde{\chi}_1^0 \tilde{\chi}_2^0$  (blue) and  $h^0 \rightarrow \tilde{\chi}_2^0 \tilde{\chi}_2^0$  (black). The parameters are chosen as in Figure 22.

particles, like  $\tilde{\chi}_{1,2}^0 l^+ l^-$  or  $\tilde{\chi}_{1,2}^0 q \bar{q}$ , become very important when the decays to scalars and pseudoscalars are kinematically forbidden.

In addition, the decays of the light Higgs boson  $h^0$  can also play a very important role in the study of the different generations, provided it can decay to final states including  $\tilde{\chi}_1^0$  or  $\tilde{\chi}_2^0$ . In this case typically the standard Higgs boson decays are reduced to less than 40%, completely changing the usual search strategies.

In Figure 23 the branching ratios of standard and exotic Higgs boson decay channels are shown. The left plot shows the suppressed branching ratio of the standard  $b\bar{b}$  channel. The main decay channel is  $\tilde{\chi}_1^0 \tilde{\chi}_1^0$ , but there is a sizeable branching ratio to  $\tilde{\chi}_1^0 \tilde{\chi}_2^0$ . Note that  $\tilde{\chi}_2^0$  decays dominantly to  $\tilde{\chi}_1^0$  plus two SM fermions. This feature allows us to distinguish between the 1  $\tilde{\nu}^c$ -model and models with more than one generation of singlets. Finally, the branching ratio to  $\tilde{\chi}_2^0 \tilde{\chi}_2^0$  is small due to kinematics, but leads to interesting final states with up to eight b-jets plus missing energy.

A final comment is in order. In these kind of scenarios with many light singlets  $\tilde{\chi}_1^0$  decays to  $\nu b\bar{b}$  can be dominant. This will reduce the available statistics in the interesting  $l_i l_j \nu$  and  $l q_i \bar{q}_j$  channels. Moreover, the correlations are less pronounced due to mixing effects in the singlet sector.



## VI. DISCUSSION AND CONCLUSIONS

We have studied the phenomenology of the  $\mu\nu$ SSM. This proposal solves at the same time the  $\mu$ -problem of the MSSM and generates small neutrino masses, consistent with data from neutrino oscillation experiments. Neutrino data put very stringent constraints on the parameter space of the model. Both the left-sneutrino vacuum expectation values and the effective bilinear parameters have to be small compared to MSSM soft SUSY breaking parameters. As a result all SUSY production cross sections and all decay chains are very similar to the NMSSM, the only, but phenomenologically very important, exceptions being the decay of the LSP and NLSP (the latter only in some parts of the parameter space) plus the decays of the lightest Higgses.

We have discussed in some details two variants of the model. In the simplest version with only one generation of singlets 1-loop corrections to the neutralino-neutrino mass matrix need to be carefully calculated in order to explain neutrino data correctly. The advantage of this minimal scheme is that effectively it contains only six new (combinations of)  $\mathcal{R}_p$  parameters, which can be fixed to a large extent by the requirement that oscillation data is correctly explained. This feature of the model is very similar to explicit bilinear R-parity breaking, although, as we have discussed, the relative importance of the different 1-loop contributions is different in the  $\mu\nu$ SSM and in bilinear  $\mathcal{R}_p$ . Certain ratios of decay branching ratios depend on the same parameter combinations as neutrino angles and are therefore predicted from neutrino physics, to a large extent independent of NMSSM parameters. We have also calculated the decay length of the LSP, which depends mostly on the LSP mass and the (experimentally determined) neutrino masses. Lengths sufficiently large to observe displaced vertices are predicted over most parts of the parameter space. However, for neutralinos lighter than approximately 30 GeV, decay lengths become larger than 10 meter, making the observation of  $\mathcal{R}_p$  difficult for LHC experiments. However, if there is a singlet scalar or pseudoscalar with a mass smaller than the lightest neutralino,  $\tilde{\chi}_1^0 \rightarrow S_m^0 (P_m^0) \nu$  is the dominant decay mode and the corresponding decay lengths become much smaller, such that the displaced vertex signature of  $\mathcal{R}_p$  might even be lost in some points of this part of parameter space. On the other hand, in case the mass of the lightest scalar is larger than twice the singlino mass, the decay  $S_m^0 \rightarrow 2\tilde{\chi}_1^0$  becomes important, both for  $S_m^0 \sim \tilde{\nu}^c$  and  $S_m^0 \sim h^0$ . If this kinematical situation is realized also the Higgs search at the LHC will definitely be affected.

The more involved  $n$  generation variants of the  $\mu\nu$ SSM can explain all neutrino data at tree-level and therefore are *calculationally* simpler. Depending on the nature of the neutralino, neutralino LSP decays show different correlations with either solar or atmospheric neutrino angles. This is guaranteed in the two generation version of the model and likely, but not always true, for  $n$  generations. If the NMSSM coupling  $\lambda$  is sufficiently small also the NLSP has decays to  $\mathcal{R}_p$  final states with potentially measurable branching ratios. In this part of parameter space it seems possible, in principle, to test both solar and atmospheric neutrino angles. If only the singlino(s) are light, i.e. the singlet scalars are heavier than, say, the  $h^0$ , the decay length of the singlino is very sharply predicted as a function of its mass and either the solar or atmospheric neutrino mass scale. If both, singlinos and singlet scalars (or pseudoscalars) are light, bino NLSP and  $h^0$  will decay not only to the lightest singlinos/singlets but also to next-to-lightest states. This leads to enhanced multiplicities in the final states and the possibility to observe multiple displaced vertices.

We now briefly discuss possible differences in collider phenomenology of the  $\mu\nu$ SSM and other R-parity breaking schemes. Different models of R-parity breaking appear clearly distinct at the Lagrangian level. However, at accelerator experiments it can be very hard to distinguish the different proposals. This can be easily understood from the fact that for a heavy singlet sector all  $\mathcal{R}_p$  models approach necessarily the MSSM with explicit R-parity breaking terms. It is therefore an interesting question to ask, what - if any - kind of signals could exist, which at least might hint at which model is the correct description of  $\mathcal{R}_p$ . Given the large variety of possibilities and the very limited predictive power of the most general cases, any discussion *before* the discovery of SUSY must be rather qualitative.

First one should mention that not all  $\mathcal{R}_p$  models explaining neutrino data show correlations between LSP decay branching ratios and neutrino angles. Especially the large number of free parameters in trilinear models exclude the possibility to make any definite predictions.  $\mathcal{R}_p$  models which do show such correlations, on the other hand, lead usually to very similar predictions for the corresponding LSP decays. For example, fitting the atmospheric data with tree-level  $\mathcal{R}_p$  terms, a bino LSP in explicit bilinear models and in the  $\mu\nu$ SSM decay with the same ratio of branching ratios into  $Wl$  (or  $lq_i\bar{q}_j$ ) final states. Thus, to distinguish the different proposals other signals are needed.

We will briefly discuss the main differences in collider phenomenology between the following three propos-

	Displaced vertex	Comment	Br(invisible)	Higgs decays
$b\text{-}\mathcal{R}_p$	Yes	Visible	$\leq 10\%$	standard
$s\text{-}\mathcal{R}_p$	Yes/No	anti-correlates with invisible	any	non-standard (invisible)
$\mu\nu\text{SSM}$	Yes/No	anti-correlates with non-standard Higgs	$\leq 10\%$	non-standard

Table III: Comparison of displaced vertex signal, completely invisible final state branching ratios for LSP decays and lightest Higgs decays for three different R-parity violating models. For a discussion see text.

als: (i) MSSM with explicit bilinear terms ( $b\text{-}\mathcal{R}_p$ ); (ii) Spontaneous  $\mathcal{R}_p$  ( $s\text{-}\mathcal{R}_p$ ) model and (iii)  $\mu\nu\text{SSM}$ . Table (III) shows a brief summary of this comparison. Differences occur in (a) the observability of a displaced vertex of the lightest neutralino decay; (b) the upper limit on the branching ratio of the lightest neutralino decaying completely invisible and (c) standard versus non-standard lightest Higgs decays.

The decay length of the lightest neutralino is fixed in both, the  $b\text{-}\mathcal{R}_p$  model and the  $\mu\nu\text{SSM}$ , essentially by the mass of the lightest neutralino and the experimentally determined neutrino masses. For  $m(\tilde{\chi}_1^0)$  larger than the W-mass decay lengths are typically of the order of  $\mathcal{O}(mm)$  and proportional to  $m^{-1}(\tilde{\chi}_1^0)$ . For lighter neutralinos, larger decay lengths are expected, see Figures 13 and 21, which scale like  $m^{-4}(\tilde{\chi}_1^0)$ . Shorter decay lengths are not possible in  $b\text{-}\mathcal{R}_p$  and possible in the  $\mu\nu\text{SSM}$  only if at least one (singlet) scalar or pseudoscalar is lighter than  $\tilde{\chi}_1^0$ , when  $\tilde{\chi}_1^0 \rightarrow S_m^0(P_m^0)\nu$  dominates. Since in the  $\mu\nu\text{SSM}$  the singlet scalars decay with a short decay length to  $\bar{b}b$ , one expects that in the  $\mu\nu\text{SSM}$  short  $\tilde{\chi}_1^0$  decay lengths correlate with the dominance of  $\bar{b}b + \text{missing energy}$  final states. In the  $s\text{-}\mathcal{R}_p$ , on the other hand, the  $\tilde{\chi}_1^0$  decay length can be shorter than in the  $b\text{-}\mathcal{R}_p$ , due to the new final state  $\tilde{\chi}_1^0 \rightarrow J + \nu$ , where  $J$  is the Majoron. Therefore, different from the  $\mu\nu\text{SSM}$ , the neutralino decay length in the  $s\text{-}\mathcal{R}_p$  model anti-correlates with the branching ratio for the invisible neutralino decay.

Finally, in the  $b\text{-}\mathcal{R}_p$  one expects that the decay properties of the lightest Higgs ( $h^0$ ) are equal to the MSSM expectations, the only exception being the case when  $h^0 \rightarrow 2\tilde{\chi}_1^0$  is possible kinematically, in which the  $\tilde{\chi}_1^0$  decays themselves can then lead to a non-standard signal in the Higgs sector. This is different in  $s\text{-}\mathcal{R}_p$ , where for a low-scale of spontaneous R-parity breaking, the  $h^0$  can decay to two Majorons, i.e. large branching ratios of Higgs to invisible particles are possible. In the  $\mu\nu\text{SSM}$  the  $h^0$  decays can be non-standard, if the lightest singlino is lighter than  $m(h^0)/2$ . However, since the singlino decay, this will not lead to an invisible Higgs, unless the mass of the singlino is so small, that the decays occur outside the detector.

To summarize this brief discussion,  $b\text{-}\mathcal{R}_p$ ,  $s\text{-}\mathcal{R}_p$  and  $\mu\nu\text{SSM}$  can, in principle, be distinguished experimentally *if the singlets are light enough to be observed* in case of  $s\text{-}\mathcal{R}_p$  and  $\mu\nu\text{SSM}$ . We note in passing that we have not found any striking differences in collider phenomenology of the  $\mu\nu\text{SSM}$  and the NMSSM with explicit bilinear terms.

In conclusion, the  $\mu\nu\text{SSM}$  offers a very rich phenomenology. Especially scenarios with light singlets deserve further, much more detailed studies.

### Acknowledgments

This work was supported by Spanish grants FPA2008-00319/FPA and Accion Integrada NO HA-2007-0090 (MEC) and by the ‘‘Fonds zur F6rderung der wissenschaftlichen Forschung (FWF)’’ of Austria, project No. P18959-N16. The authors acknowledge support from EU under the MRTN-CT-2006-025505 and MTRN-CT-2006-503369 network programmes. A.B. was supported by the Spanish grants SAB 2006-0072, FPA 2005-01269, FPA 2005-25348-E and FPA 2008-00319/FPA of the Ministerio de Education y Ciencia. A.V. thanks the Generalitat Valenciana for financial support. W.P. and S.L. are supported by the DAAD, project number D/07/13468 and by the Initiative and Networking Fund of the Helmholtz Association, contract HA-101 (‘‘Physics at the Terascale’’).

## Appendix A: MASS MATRICES

In the scalar mass matrices shown below the tadpole equations have not yet been used to reduce the number of free parameters.

### 1. Charged Scalars

In the basis

$$\begin{aligned} (S^{+'})^T &= ((H_d^-)^*, H_u^+, \tilde{e}_L^*, \tilde{\mu}_L^*, \tilde{\tau}_L^*, \tilde{e}_R, \tilde{\mu}_R, \tilde{\tau}_R) \\ (S^{-'})^T &= (H_d^-, (H_u^+)^*, \tilde{e}_L, \tilde{\mu}_L, \tilde{\tau}_L, \tilde{e}_R^*, \tilde{\mu}_R^*, \tilde{\tau}_R^*) \end{aligned} \quad (\text{A1})$$

the scalar potential includes the term

$$V \supset (S^{-'})^T M_{S^\pm}^2 S^{+'} \quad , \quad (\text{A2})$$

where  $M_{S^\pm}^2$  is the  $(8 \times 8)$  mass matrix of the charged scalars. In the  $\xi = 0$  gauge it can be written as

$$M_{S^\pm}^2 = \begin{pmatrix} M_{HH}^2 & (M_{H\bar{l}}^2)^\dagger \\ M_{H\bar{l}}^2 & M_{\bar{l}\bar{l}}^2 \end{pmatrix} \quad . \quad (\text{A3})$$

The  $(2 \times 2)$   $M_{HH}^2$  matrix is given by:

$$\begin{aligned} (M_{HH}^2)_{11} &= m_{H_d}^2 + \frac{1}{8}[(g^2 + g'^2)v_d^2 + (g^2 - g'^2)(v_u^2 - v_1^2 - v_2^2 - v_3^2)] \\ &\quad + \frac{1}{2}\lambda_s\lambda_t^*v_{R_s}v_{R_t} + \frac{1}{2}v_i(h_E h_E^\dagger)_{ij}v_j \\ (M_{HH}^2)_{12} &= \frac{1}{4}g^2v_uv_d - \frac{1}{2}\lambda_s\lambda_s^*v_uv_d + \frac{1}{4}\lambda_s\kappa_s^*v_{R_s}^2 + \frac{1}{2}v_uv_i\lambda_s(h_\nu^{is})^* + \frac{1}{\sqrt{2}}v_{R_s}T_\lambda^s \\ (M_{HH}^2)_{21} &= (M_{HH}^2)_{12}^* \\ (M_{HH}^2)_{22} &= m_{H_u}^2 + \frac{1}{8}[(g^2 + g'^2)v_u^2 + (g^2 - g'^2)(v_d^2 + v_1^2 + v_2^2 + v_3^2)] \\ &\quad + \frac{1}{2}\lambda_s\lambda_t^*v_{R_s}v_{R_t} + \frac{1}{2}v_{R_s}v_{R_t}h_\nu^{is}(h_\nu^{it})^* \end{aligned} \quad (\text{A4})$$

The  $(6 \times 2)$  matrix that mixes the charged Higgs bosons with the charged sleptons is

$$M_{H\bar{l}}^2 = \begin{pmatrix} M_{HL}^2 \\ M_{HR}^2 \end{pmatrix} \quad (\text{A5})$$

with:

$$\begin{aligned} (M_{HL}^2)_{i1} &= \frac{1}{4}g^2v_dv_i - \frac{1}{2}\lambda_s^*h_\nu^{it}v_{R_s}v_{R_t} - \frac{1}{2}v_d(h_E h_E^\dagger)_{ij}v_j \\ (M_{HL}^2)_{i2} &= \frac{1}{4}g^2v_uv_i - \frac{1}{4}\kappa_s^*v_{R_s}^2h_\nu^{is} + \frac{1}{2}v_uv_d\lambda_s^*h_\nu^{is} - \frac{1}{2}v_uv_jh_\nu^{is}(h_\nu^{js})^* - \frac{1}{\sqrt{2}}v_{R_s}T_{h_\nu}^{is} \\ (M_{HR}^2)_{i1} &= -\frac{1}{2}v_uv_{R_s}(h_E^*)_{ji}h_\nu^{js} - \frac{1}{\sqrt{2}}v_j(T_E^*)_{ji} \\ (M_{HR}^2)_{i2} &= -\frac{1}{2}\lambda_s v_{R_s}v_j(h_E^*)_{ji} - \frac{1}{2}v_d(h_E^*)_{ji}h_\nu^{js}v_{R_s} \end{aligned} \quad (\text{A6})$$

Finally, the  $(6 \times 6)$  mass matrix of the charged sleptons can be written as

$$M_{\tilde{l}}^2 = \begin{pmatrix} M_{LL}^2 & M_{LR}^2 \\ M_{RL}^2 & M_{RR}^2 \end{pmatrix} \quad (\text{A7})$$

with:

$$\begin{aligned} (M_{LL}^2)_{ij} &= (m_L^2)_{ij} + \frac{1}{8}(g'^2 - g^2)(v_d^2 - v_u^2 + v_1^2 + v_2^2 + v_3^2)\delta_{ij} + \frac{1}{4}g^2 v_i v_j \\ &\quad + \frac{1}{2}v_d^2 (h_E h_E^\dagger)_{ij} + \frac{1}{2}v_{Rs} v_{Rt} h_\nu^{is} (h_\nu^{jt})^* \\ M_{LR}^2 &= -\frac{1}{2}\lambda_s^* v_{Rs} v_u h_E + \frac{1}{\sqrt{2}}v_d T_E \\ M_{RL}^2 &= (M_{LR}^2)^\dagger \\ (M_{RR}^2)_{ij} &= (m_R^2)_{ij} + \frac{1}{4}g'^2(v_u^2 - v_d^2 - v_1^2 - v_2^2 - v_3^2)\delta_{ij} \\ &\quad + \frac{1}{2}v_d^2 (h_E^\dagger h_E)_{ij} + \frac{1}{2}v_k v_m (h_E^\dagger)_{ik} (h_E)_{mj} \end{aligned} \quad (\text{A8})$$

## 2. Neutral Scalars

In the basis

$$(S^{0'})^T = \text{Re}(H_d^0, H_u^0, \tilde{\nu}_s^c, \tilde{\nu}_i) \quad (\text{A9})$$

the scalar potential includes the term

$$V \supset (S^{0'})^T M_{S^0}^2 S^{0'} \quad (\text{A10})$$

and the  $((5+n) \times (5+n))$  neutral scalar mass matrix can be written as

$$M_{S^0}^2 = \begin{pmatrix} M_{HH}^2 & M_{HS}^2 & M_{H\tilde{L}}^2 \\ (M_{HS}^2)^T & M_{SS}^2 & M_{\tilde{L}S}^2 \\ (M_{H\tilde{L}}^2)^T & (M_{\tilde{L}S}^2)^T & M_{\tilde{L}\tilde{L}}^2 \end{pmatrix}. \quad (\text{A11})$$

The matrix elements are given as follows:

$$\begin{aligned} (M_{HH}^2)_{11} &= m_{H_d}^2 + \frac{1}{8}(g^2 + g'^2)(3v_d^2 - v_u^2 + v_1^2 + v_2^2 + v_3^2) \\ &\quad + \frac{1}{2}\lambda_s \lambda_t^* v_{Rs} v_{Rt} + \frac{1}{2}v_u^2 \lambda_s \lambda_s^* \\ (M_{HH}^2)_{12} &= -\frac{1}{4}(g^2 + g'^2)v_d v_u + \lambda_s \lambda_s^* v_d v_u - \frac{1}{8}v_{Rs}^2 (\lambda_s \kappa_s^* + h.c.) \\ &\quad - \frac{1}{2}v_u v_i (\lambda_s^* h_\nu^{is} + h.c.) - \frac{1}{2\sqrt{2}}v_{Rs} (T_\lambda^s + h.c.) \\ (M_{HH}^2)_{21} &= (M_{HH}^2)_{12} \\ (M_{HH}^2)_{22} &= m_{H_u}^2 - \frac{1}{8}(g^2 + g'^2)(v_d^2 - 3v_u^2 + v_1^2 + v_2^2 + v_3^2) \\ &\quad + \frac{1}{2}\lambda_s \lambda_t^* v_{Rs} v_{Rt} + \frac{1}{2}v_d^2 \lambda_s \lambda_s^* + \frac{1}{2}v_{Rs} v_{Rt} h_\nu^{is} (h_\nu^{it})^* + \frac{1}{2}v_i v_j (h_\nu^{is})^* h_\nu^{js} \\ &\quad - \frac{1}{2}v_d v_i (\lambda_s^* h_\nu^{is} + h.c.) \end{aligned} \quad (\text{A12})$$

$$\begin{aligned}
(M_{HS}^2)_{1s} &= -\frac{1}{4}v_u v_{Rs}(\lambda_s^* \kappa_s + h.c.) + \frac{1}{2}v_d v_{Rt}(\lambda_s \lambda_t^* + h.c.) \\
&\quad - \frac{1}{2\sqrt{2}}v_u(T_\lambda^s + h.c.) - \frac{1}{4}v_i v_{Rt}(\lambda_s^* h_\nu^{it} + \lambda_t^* h_\nu^{is} + h.c.) \\
(M_{HS}^2)_{2s} &= -\frac{1}{4}v_d v_{Rs}(\lambda_s^* \kappa_s + h.c.) + \frac{1}{2}v_u v_{Rt}(\lambda_s \lambda_t^* + h.c.) \\
&\quad - \frac{1}{2\sqrt{2}}v_d(T_\lambda^s + h.c.) + \frac{1}{2\sqrt{2}}v_t(T_{h_\nu}^{ts} + h.c.) + \frac{1}{4}v_{Rs}v_i(\kappa_s^* h_\nu^{is} + h.c.) \\
&\quad + \frac{1}{2}v_u v_{Rt}[h_\nu^{is}(h_\nu^{it})^* + h.c.]
\end{aligned} \tag{A13}$$

$$\begin{aligned}
(M_{HL}^2)_{1i} &= \frac{1}{4}(g^2 + g'^2)v_d v_i - \frac{1}{4}v_u^2(\lambda_s^* h_\nu^{is} + h.c.) - \frac{1}{4}v_{Rs}v_{Rt}(\lambda_s^* h_\nu^{it} + h.c.) \\
(M_{HL}^2)_{2i} &= -\frac{1}{4}(g^2 + g'^2)v_u v_i + \frac{1}{8}v_{Rs}^2(\kappa_s^* h_\nu^{is} + h.c.) - \frac{1}{2}v_u v_d(\lambda_s^* h_\nu^{is} + h.c.) \\
&\quad + \frac{1}{2}v_u v_j[h_\nu^{js}(h_\nu^{is})^* + h.c.] + \frac{1}{2\sqrt{2}}v_{Rs}(T_{h_\nu}^{is} + h.c.)
\end{aligned} \tag{A14}$$

$$\begin{aligned}
(M_{SS}^2)_{st} &= \frac{1}{2}[(m_{\nu^c}^2)_{st} + (m_{\nu^c}^2)_{ts}] + \frac{1}{4}(\lambda_s \lambda_t^* + h.c.)(v_d^2 + v_u^2) - \frac{1}{4}v_d v_u(\lambda_s^* \kappa_s + h.c.)\delta_{st} \\
&\quad + \frac{3}{4}\kappa_s \kappa_s^* v_{Rs}^2 \delta_{st} + \frac{1}{4}v_u v_i(\kappa_s^* h_\nu^{is} + h.c.)\delta_{st} + \frac{1}{4}v_u^2[(h_\nu^{is})^* h_\nu^{it} + h.c.] \\
&\quad + \frac{1}{4}v_i v_j[(h_\nu^{is})^* h_\nu^{jt} + h.c.] - \frac{1}{4}v_d v_i[\lambda_s^* h_\nu^{it} + \lambda_t(h_\nu^{is})^* + h.c.] \\
&\quad + \frac{1}{2\sqrt{2}}v_{Ru}(T_\kappa^{stu} + h.c.)
\end{aligned} \tag{A15}$$

$$\begin{aligned}
(M_{LS}^2)_{si} &= \frac{1}{4}v_u v_{Rs}(\kappa_s^* h_\nu^{is} + h.c.) - \frac{1}{4}v_d v_{Rt}(\lambda_s^* h_\nu^{it} + \lambda_t^* h_\nu^{is} + h.c.) \\
&\quad + \frac{1}{2\sqrt{2}}v_u(T_{h_\nu}^{is} + h.c.) + \frac{1}{4}v_j v_{Rt}[h_\nu^{jt}(h_\nu^{is})^* + h_\nu^{js}(h_\nu^{it})^* + h.c.]
\end{aligned} \tag{A16}$$

$$\begin{aligned}
(M_{LL}^2)_{ij} &= \frac{1}{2}[(m_L^2)_{ij} + (m_L^2)_{ji}] + \frac{1}{8}(g^2 + g'^2)(v_d^2 - v_u^2 + v_1^2 + v_2^2 + v_3^2)\delta_{ij} \\
&\quad + \frac{1}{4}(g^2 + g'^2)v_i v_j + \frac{1}{4}v_u^2[h_\nu^{is}(h_\nu^{js})^* + h.c.] + \frac{1}{4}v_{Rs}v_{Rt}[h_\nu^{is}(h_\nu^{jt})^* + h.c.]
\end{aligned} \tag{A17}$$

### 3. Pseudoscalars

In the basis

$$(P^{0'})^T = Im(H_d^0, H_u^0, \tilde{\nu}_s^c, \tilde{\nu}_i) \tag{A18}$$

the scalar potential includes the term

$$V \supset (P^{0'})^T M_{P^0}^2 P^{0'} \tag{A19}$$

and the  $((5+n) \times (5+n))$  pseudoscalar mass matrix can be written as

$$M_{P^0}^2 = \begin{pmatrix} M_{HH}^2 & M_{HS}^2 & M_{HL}^2 \\ (M_{HS}^2)^T & M_{SS}^2 & M_{LS}^2 \\ (M_{HL}^2)^T & (M_{LS}^2)^T & M_{LL}^2 \end{pmatrix}. \tag{A20}$$

The matrix elements are given as follows:

$$\begin{aligned}
(M_{HH}^2)_{11} &= m_{H_d}^2 + \frac{1}{8}(g^2 + g'^2)(v_d^2 - v_u^2 + v_1^2 + v_2^2 + v_3^2) \\
&\quad + \frac{1}{2}\lambda_s\lambda_t^*v_{R_s}v_{R_t} + \frac{1}{2}v_u^2\lambda_s\lambda_s^* \\
(M_{HH}^2)_{12} &= \frac{1}{8}v_{R_s}^2(\lambda_s\kappa_s^* + h.c.) + \frac{1}{2\sqrt{2}}v_{R_s}(T_\lambda^s + h.c.) \\
(M_{HH}^2)_{21} &= (M_{HH}^2)_{12} \\
(M_{HH}^2)_{22} &= m_{H_u}^2 - \frac{1}{8}(g^2 + g'^2)(v_d^2 - v_u^2 + v_1^2 + v_2^2 + v_3^2) \\
&\quad + \frac{1}{2}\lambda_s\lambda_t^*v_{R_s}v_{R_t} + \frac{1}{2}v_d^2\lambda_s\lambda_s^* + \frac{1}{2}v_{R_s}v_{R_t}h_\nu^{is}(h_\nu^{it})^* + \frac{1}{2}v_i v_j (h_\nu^{is})^* h_\nu^{js} \\
&\quad - \frac{1}{2}v_d v_i (\lambda_s^* h_\nu^{is} + h.c.)
\end{aligned} \tag{A21}$$

$$\begin{aligned}
(M_{HS}^2)_{1s} &= -\frac{1}{4}v_u v_{R_s}(\lambda_s^* \kappa_s + h.c.) + \frac{1}{4} \sum_{t \neq s} v_i v_{R_t}(\lambda_s^* h_\nu^{it} - \lambda_t^* h_\nu^{is} + h.c.) \\
&\quad + \frac{1}{2\sqrt{2}}v_u(T_\lambda^s + h.c.) \\
(M_{HS}^2)_{2s} &= -\frac{1}{4}v_d v_{R_s}(\lambda_s^* \kappa_s + h.c.) + \frac{1}{4}v_{R_s}v_i(\kappa_s^* h_\nu^{is} + h.c.) \\
&\quad + \frac{1}{2\sqrt{2}}v_d(T_\lambda^s + h.c.) - \frac{1}{2\sqrt{2}}v_i(T_{h_\nu}^{is} + h.c.)
\end{aligned} \tag{A22}$$

$$\begin{aligned}
(M_{H\bar{L}}^2)_{1i} &= -\frac{1}{4}v_u^2(\lambda_s^* h_\nu^{is} + h.c.) - \frac{1}{4}v_{R_s}v_{R_t}(\lambda_s^* h_\nu^{it} + h.c.) \\
(M_{H\bar{L}}^2)_{2i} &= -\frac{1}{8}v_{R_s}^2(\kappa_s^* h_\nu^{is} + h.c.) - \frac{1}{2\sqrt{2}}v_{R_s}(T_{h_\nu}^{is} + h.c.)
\end{aligned} \tag{A23}$$

$$\begin{aligned}
(M_{SS}^2)_{st} &= \frac{1}{2}[(m_{\bar{\nu}^c}^2)_{st} + (m_{\bar{\nu}^c}^2)_{ts}] + \frac{1}{4}(\lambda_s\lambda_t^* + h.c.)(v_d^2 + v_u^2) + \frac{1}{4}v_d v_u (\lambda_s^* \kappa_s + h.c.) \delta_{st} \\
&\quad + \frac{1}{4}\kappa_s\kappa_s^*v_{R_s}^2\delta_{st} - \frac{1}{4}v_u v_i (\kappa_s^* h_\nu^{is} + h.c.) \delta_{st} + \frac{1}{4}v_u^2[(h_\nu^{is})^* h_\nu^{it} + h.c.] \\
&\quad + \frac{1}{4}v_i v_j [(h_\nu^{is})^* h_\nu^{jt} + h.c.] - \frac{1}{4}v_d v_i [\lambda_s^* h_\nu^{it} + \lambda_t (h_\nu^{is})^* + h.c.] \\
&\quad - \frac{1}{2\sqrt{2}}v_{R_u}(T_\kappa^{st} + h.c.)
\end{aligned} \tag{A24}$$

$$\begin{aligned}
(M_{\bar{L}S}^2)_{si} &= \frac{1}{4}v_u v_{R_s}(\kappa_s^* h_\nu^{is} + h.c.) + \frac{1}{4} \sum_{t \neq s} v_d v_{R_t}(\lambda_t^* h_\nu^{is} - \lambda_s^* h_\nu^{it} + h.c.) \\
&\quad + \frac{1}{4} \sum_{t \neq s} v_j v_{R_t} [h_\nu^{js} (h_\nu^{it})^* - h_\nu^{jt} (h_\nu^{is})^* + h.c.] - \frac{1}{2\sqrt{2}}v_u(T_{h_\nu}^{is} + h.c.)
\end{aligned} \tag{A25}$$

$$\begin{aligned}
(M_{\bar{L}\bar{L}}^2)_{ij} &= \frac{1}{2}[(m_{\bar{L}}^2)_{ij} + (m_{\bar{L}}^2)_{ji}] + \frac{1}{8}(g^2 + g'^2)(v_d^2 - v_u^2 + v_1^2 + v_2^2 + v_3^2)\delta_{ij} \\
&\quad + \frac{1}{4}v_u^2[h_\nu^{is}(h_\nu^{js})^* + h.c.] + \frac{1}{4}v_{R_s}v_{R_t}[h_\nu^{is}(h_\nu^{jt})^* + h.c.]
\end{aligned} \tag{A26}$$

#### 4. Neutral Fermions

In the basis

$$(\psi^0)^T = (\tilde{B}^0, \tilde{W}_3^0, \tilde{H}_d^0, \tilde{H}_u^0, \nu_s^c, \nu_i) \quad (\text{A27})$$

the lagrangian of the model includes the term

$$\mathcal{L} \supset -\frac{1}{2}(\psi^0)^T \mathcal{M}_n \psi^0 + h.c. \quad (\text{A28})$$

with the  $((7+n) \times (7+n))$  mass matrix of the neutral fermions, which can be written as:

$$\mathcal{M}_n = \begin{pmatrix} M_{\tilde{\chi}^0} & m_{\tilde{\chi}^0 \nu^c} & m_{\tilde{\chi}^0 \nu} \\ m_{\tilde{\chi}^0 \nu^c}^T & M_R & m_D \\ m_{\tilde{\chi}^0 \nu}^T & m_D^T & 0 \end{pmatrix} \quad (\text{A29})$$

$M_{\tilde{\chi}^0}$  is the usual mass matrix of the neutralinos in the MSSM

$$M_{\tilde{\chi}^0} = \begin{pmatrix} M_1 & 0 & -\frac{1}{2}g'v_d & \frac{1}{2}g'v_u \\ 0 & M_2 & \frac{1}{2}g'v_d & -\frac{1}{2}g'v_u \\ -\frac{1}{2}g'v_d & \frac{1}{2}g'v_d & 0 & -\mu \\ \frac{1}{2}g'v_u & -\frac{1}{2}g'v_u & -\mu & 0 \end{pmatrix} \quad (\text{A30})$$

with

$$\mu = \frac{1}{\sqrt{2}}\lambda_s v_{Rs} \quad . \quad (\text{A31})$$

The mixing between the neutralinos and the singlet  $\nu_s^c$  is given by

$$(m_{\tilde{\chi}^0 \nu^c}^T)_s = \left( 0 \ 0 \ -\frac{1}{\sqrt{2}}\lambda_s v_u \ -\frac{1}{\sqrt{2}}\lambda_s v_d + \frac{1}{\sqrt{2}}v_i h_\nu^{is} \right) \quad . \quad (\text{A32})$$

$m_{\tilde{\chi}^0 \nu}$  is the neutralino-neutrino mixing part

$$m_{\tilde{\chi}^0 \nu}^T = \begin{pmatrix} -\frac{1}{2}g'v_1 & \frac{1}{2}g'v_1 & 0 & \epsilon_1 \\ -\frac{1}{2}g'v_2 & \frac{1}{2}g'v_2 & 0 & \epsilon_2 \\ -\frac{1}{2}g'v_3 & \frac{1}{2}g'v_3 & 0 & \epsilon_3 \end{pmatrix} \quad (\text{A33})$$

with

$$\epsilon_i = \frac{1}{\sqrt{2}} \sum_{s=1}^n v_{Rs} h_\nu^{is} \quad . \quad (\text{A34})$$

The neutrino Dirac term is

$$(m_D)_{is} = \frac{1}{\sqrt{2}} h_\nu^{is} v_u \quad (\text{A35})$$

and finally  $M_R$  is

$$(M_R)_{st} = \frac{1}{\sqrt{2}} \kappa_s v_{Rs} \delta_{st} \quad . \quad (\text{A36})$$

## 5. Charged Fermions

In the basis

$$\begin{aligned} (\psi^-)^T &= (\tilde{W}^-, \tilde{H}_d^-, e, \mu, \tau) \\ (\psi^+)^T &= (\tilde{W}^+, \tilde{H}_u^+, e^c, \mu^c, \tau^c), \end{aligned} \quad (\text{A37})$$

the  $(5 \times 5)$  mass matrix of the charged fermions is given by

$$\mathcal{M}_c = \begin{pmatrix} M_2 & \frac{1}{\sqrt{2}}gv_u & 0 & 0 & 0 \\ \frac{1}{\sqrt{2}}gv_d & \mu & -\frac{1}{\sqrt{2}}h_E^{i1}v_i & -\frac{1}{\sqrt{2}}h_E^{i2}v_i & -\frac{1}{\sqrt{2}}h_E^{i3}v_i \\ \frac{1}{\sqrt{2}}gv_1 & -\epsilon_1 & \frac{1}{\sqrt{2}}h_E^{11}v_d & 0 & 0 \\ \frac{1}{\sqrt{2}}gv_2 & -\epsilon_2 & 0 & \frac{1}{\sqrt{2}}h_E^{22}v_d & 0 \\ \frac{1}{\sqrt{2}}gv_3 & -\epsilon_3 & 0 & 0 & \frac{1}{\sqrt{2}}h_E^{33}v_d \end{pmatrix}. \quad (\text{A38})$$

### Appendix B: COUPLING $\tilde{\chi}_1^0 - W^\pm - l_i^\mp$

Approximate formulas for the coupling  $\tilde{\chi}_1^0 - W^\pm - l_i^\mp$  can be obtained from the general  $\tilde{\chi}_i^0 - W^\pm - \tilde{\chi}_j^\mp$  interaction lagrangian

$$\mathcal{L} \supset \overline{\tilde{\chi}_i^0} \gamma^\mu (O_{Lij}^{cnw} P_L + O_{Rij}^{cnw} P_R) \tilde{\chi}_j^0 W_\mu^- + \overline{\tilde{\chi}_i^0} \gamma^\mu (O_{Lij}^{ncw} P_L + O_{Rij}^{ncw} P_R) \tilde{\chi}_j^- W_\mu^+ \quad , \quad (\text{B1})$$

where

$$\begin{aligned} O_{Li1}^{cnw} &= g \left[ -\mathcal{U}_{i1} \mathcal{N}_{12}^* - \frac{1}{\sqrt{2}} \left( \mathcal{U}_{i2} \mathcal{N}_{13}^* + \sum_{k=1}^3 \mathcal{U}_{i,2+k} \mathcal{N}_{1,5+k}^* \right) \right] \\ O_{Ri1}^{cnw} &= g \left( -\mathcal{V}_{i1}^* \mathcal{N}_{12} + \frac{1}{\sqrt{2}} \mathcal{V}_{i2}^* \mathcal{N}_{14} \right) \\ O_{L1j}^{ncw} &= (O_{Lj1}^{cnw})^* \\ O_{R1j}^{ncw} &= (O_{Rj1}^{cnw})^* \quad . \end{aligned} \quad (\text{B2})$$

The matrix  $\mathcal{N}$  diagonalizes the neutral fermion mass matrix (see Appendix (A 4)) while the matrices  $\mathcal{U}$  and  $\mathcal{V}$  diagonalize the charged fermion mass matrix (see Appendix (A 5)).

As was already mentioned for the case of neutral fermions in Section II E, it is possible to diagonalize the mass matrices in very good approximation due to the fact that the  $\mathcal{R}_p$  parameters are small. Defining the matrices  $\xi$ ,  $\xi_L$  and  $\xi_R$ , that will be taken as expansion parameters, one gets the leading order expressions

$$\mathcal{N} = \begin{pmatrix} N & N\xi^T \\ -V^T\xi & V^T \end{pmatrix}, \quad \mathcal{U} = \begin{pmatrix} U_c & U_c\xi_L^T \\ -\xi_L & I_3 \end{pmatrix}, \quad \mathcal{V} = \begin{pmatrix} V_c & V_c\xi_R^T \\ -\xi_R & I_3 \end{pmatrix} \quad , \quad (\text{B3})$$

where  $I_3$  is the  $(3 \times 3)$  identity matrix. The expansion matrices  $\xi_L$  and  $\xi_R$  are

$$\begin{aligned} (\xi_L)_{i1} &= \frac{g\Lambda_i}{\sqrt{2}Det_+} \\ (\xi_L)_{i2} &= -\frac{\epsilon_i}{\mu} - \frac{g^2v_u\Lambda_i}{2\mu Det_+} \\ (\xi_R)_{i1} &= \frac{gv_d h_E^{ii}}{2Det_+} \left[ \frac{v_u\epsilon_i}{\mu} + \frac{(2\mu^2 + g^2v_u^2)\Lambda_i}{2\mu Det_+} \right] \\ (\xi_R)_{i2} &= -\frac{\sqrt{2}v_d h_E^{ii}}{2Det_+} \left[ \frac{M_2\epsilon_i}{\mu} + \frac{g^2(v_d\mu + M_2v_u)\Lambda_i}{2\mu Det_+} \right] \quad , \end{aligned} \quad (\text{B4})$$



where  $Det_+ = -\frac{1}{2}g^2v_d v_u + M_2\mu$  is the determinant of the MSSM chargino mass matrix,  $\mu = \frac{1}{\sqrt{2}}\lambda_s v_{Rs}$  and  $\epsilon_i = \frac{1}{\sqrt{2}}v_{Rs}h_\nu^{is}$ . The expressions for the matrix  $\xi$  depend on the number of singlet generations in the model. Particular cases can be found in (31) and (39).

Using the previous equations and assuming that all parameters are real, one gets the approximate formulas

$$\begin{aligned} O_{Li1}^{cnw} &= \frac{g}{\sqrt{2}} \left[ \frac{gN_{12}\Lambda_i}{Det_+} - \left( \frac{\epsilon_i}{\mu} + \frac{g^2v_u\Lambda_i}{2\mu Det_+} \right) N_{13} - \sum_{k=1}^n N_{1k}\xi_{ik} \right] \\ O_{Ri1}^{cnw} &= \frac{1}{2}g(h_E)_{ii} \frac{v_d}{Det_+} \left[ \frac{gv_u N_{12} - M_2 N_{14}}{\mu} \epsilon_i + \frac{g(2\mu^2 + g^2v_u^2)N_{12} - g^2(v_d\mu + M_2v_u)N_{14}}{2\mu Det_+} \Lambda_i \right] \\ O_{Li1}^{ncw} &= (O_{Li1}^{cnw})^* \\ O_{Ri1}^{ncw} &= (O_{Ri1}^{cnw})^* \end{aligned} \quad . \quad (B5)$$

It is important to emphasize that all previous formulas, and the following simplified versions, are tree-level results. More simplified formulas are possible if the lightest neutralino has a large component in one of the gauge eigenstates. These particular limits are of great interest to understand the phenomenology:

### Bino-like $\tilde{\chi}_1^0$

This limit is characterized by  $N_{11}^2 = 1$  and  $N_{1m} = 0$  for  $m \neq 1$ . One gets

$$\begin{aligned} O_{Li1}^{cnw} &= -\frac{g}{\sqrt{2}}\xi_{i1} \\ O_{Ri1}^{cnw} &= 0 \end{aligned} \quad . \quad (B6)$$

For the 1  $\hat{\nu}^c$ -model this implies that a bino-like  $\tilde{\chi}_1^0$  couples to  $Wl_i$  proportionally to  $\Lambda_i$ , see Equation (31), without any dependence on the  $\epsilon_i$  parameters.

On the other hand, for the 2  $\hat{\nu}^c$ -model, the more complicated structure of the  $\xi$  matrix, see Equations (39) and (43), implies a coupling of a bino-like  $\tilde{\chi}_1^0$  with  $Wl_i$  dependent on two pieces, one proportional to  $\Lambda_i$  and one proportional to  $\alpha_i$ :

$$\xi_{i1} = \frac{2g'M_2\mu}{m_\gamma} (a\Lambda_i + b\alpha_i) \quad (B7)$$

However, a simple estimate of the relative importance of these two terms is possible. By assuming that all masses are at the same scale  $m_{SUSY}$ , the couplings  $\kappa$  and  $\lambda$  are of order 0.1, and the  $\mathbb{R}_p$  terms  $h_\nu^i$  and  $v_i$  are of order  $h_{\mathbb{R}_p}$  and  $m_{SUSY}h_{\mathbb{R}_p}$  respectively, one can show that  $a\Lambda_i \sim 200b\alpha_i$ . Therefore, one gets a coupling which is proportional, in very good approximation, to  $\Lambda_i$ , as confirmed by the exact numerical results shown in the main part of the paper. Similar arguments apply for models with more generations of right-handed neutrinos.

In conclusion, for a bino-like neutralino the coupling  $\tilde{\chi}_1^0 - W^\pm - l_i^\mp$  is proportional to  $\Lambda_i$  to a good approximation.

### Higgsino-like $\tilde{\chi}_1^0$

This limit is characterized by  $N_{13}^2 + N_{14}^2 = 1$  and  $N_{1m} = 0$  for  $m \neq 3, 4$ . If the coupling  $O_{Ri1}^{cnw}$  is neglected due to the suppression given by the charged lepton Yukawa couplings, one gets

$$\begin{aligned} O_{Li1}^{cnw} &= -\frac{g}{\sqrt{2}} \left[ \left( \frac{\epsilon_i}{\mu} + \frac{g^2v_u\Lambda_i}{2\mu Det_+} + \xi_{i3} \right) N_{13} + \xi_{i4} N_{14} \right] \\ O_{Ri1}^{cnw} &\simeq 0 \end{aligned} \quad . \quad (B8)$$

Equations (31) and (39) show that the  $\epsilon_i$  terms cancel out in the coupling (B8), and therefore one gets dependence only on  $\Lambda_i$  in the 1  $\hat{\nu}^c$ -model, and  $(\Lambda_i, \alpha_i)$  in the 2  $\hat{\nu}^c$ -model. However, this cancellation is not perfect in  $O_{Ri1}^{cnw}$  and thus one still has some dependence on  $\epsilon_i$ .

Singlino-like  $\tilde{\chi}_1^0$ 

The limit in which the right-handed neutrino  $\nu_s^c$  is the lightest neutralino is characterized by  $N_{1m}^2 = 1$  for  $m \geq 5$  and  $N_{1l} = 0$  for  $l \neq m$ . One gets

$$\begin{aligned} O_{Li1}^{cnw} &= -\frac{g}{\sqrt{2}}\xi_{im} \\ O_{Ri1}^{cnw} &= 0 \quad . \end{aligned} \quad (\text{B9})$$

For the 1  $\hat{\nu}^c$ -model this expression implies that a pure singlino-like  $\tilde{\chi}_1^0$  couples to  $Wl_i$  proportional to  $\Lambda_i$ , see Equation (31), without any dependence on the  $\epsilon_i$  parameters. This proportionality to  $\Lambda_i$  is different to what is found in spontaneous R-parity violation, where the different structure of the corresponding  $\xi$  matrix [73] implies that the singlino couples to  $Wl_i$  proportionally to  $\epsilon_i$ .

For the  $n$   $\hat{\nu}^c$ -model one finds that the coupling  $\tilde{\chi}_1^0 - W^\pm - l_i^\mp$  for a singlino-like neutralino has little dependence on  $\Lambda_i$ . For example, in the 2  $\hat{\nu}^c$ -model one finds that the element  $\xi_{i5}$ , corresponding to the right-handed neutrino  $\nu_1^c$ , is given by

$$\xi_{i5} = \frac{M_{R2}\lambda_1 m_\gamma}{4\sqrt{2}Det(M_H)}(v_u^2 - v_d^2)\Lambda_i - \left( \sqrt{2}\lambda_2 c + \frac{4Det_0 v_{R1}}{\mu m_\gamma (v_u^2 - v_d^2)} b \right) \alpha_i \quad . \quad (\text{B10})$$

The coupling has two pieces, one proportional to  $\Lambda_i$  and one proportional to  $\alpha_i$ . However, the  $\alpha_i$  piece gives the dominant contribution, as can be shown using an estimate completely analogous to the one done for a bino-like  $\tilde{\chi}_1^0$ . In this case, the ratio between the two terms in Equation (B10) is  $\alpha_i$ -piece  $\sim 8$   $\Lambda_i$ -piece, sufficient to ensure a very good proportionality to the  $\alpha_i$  parameters. This estimate has been corroborated numerically.

- 
- [1] For an introduction to Supersymmetry and the MSSM see, for example: S. P. Martin, [arXiv:hep-ph/9709356]; I. J. R. Aitchison, [arXiv:hep-ph/0505105].
  - [2] G. R. Farrar and P. Fayet, Phys. Lett. B **76**, 575 (1978).
  - [3] S. Weinberg, Phys. Rev. D **26**, 287 (1982).
  - [4] N. Sakai and T. Yanagida, Nucl. Phys. B **197**, 533 (1982).
  - [5] Y. Fukuda *et al.* [Super-Kamiokande Collaboration], Phys. Rev. Lett. **81**, 1562 (1998)
  - [6] SNO, Q. R. Ahmad *et al.*, Phys. Rev. Lett. **89**, 011301 (2002), [nucl-ex/0204008].
  - [7] KamLAND, K. Eguchi *et al.*, Phys. Rev. Lett. **90**, 021802 (2003), [hep-ex/0212021].
  - [8] Y. Ashie *et al.* [Super-Kamiokande Collaboration], Phys. Rev. Lett. **93**, 101801 (2004) [arXiv:hep-ex/0404034].
  - [9] KamLAND collaboration, S. Abe *et al.*, arXiv:0801.4589 [hep-ex].
  - [10] J. Hosaka *et al.* [Super-Kamiokande Collaboration], Phys. Rev. D **74**, 032002 (2006) [arXiv:hep-ex/0604011].
  - [11] P. Adamson *et al.* [MINOS Collaboration], Phys. Rev. Lett. **101**, 131802 (2008) [arXiv:0806.2237 [hep-ex]].
  - [12] T. Schwetz, M. Tortola and J. W. F. Valle, New J. Phys. **10**, 113011 (2008) [arXiv:0808.2016 [hep-ph]].
  - [13] S. Weinberg, Phys. Rev. Lett. **43**, 1566 (1979); S. Weinberg, Phys. Rev. D **22**, 1694 (1980).
  - [14] P. Minkowski, Phys. Lett. B **67** (1977) 421.
  - [15] T. Yanagida, in *KEK lectures*, ed. O. Sawada and A. Sugamoto, KEK, 1979; M Gell-Mann, P Ramond, R. Slansky, in *Supergravity*, ed. P. van Nieuwenhuizen and D. Freedman (North Holland, 1979);
  - [16] R.N. Mohapatra and G. Senjanovic, Phys. Rev. Lett. **44** 912 (1980).
  - [17] J. Schechter and J. W. F. Valle, Phys. Rev. D **22**, 2227 (1980).
  - [18] T. P. Cheng and L. F. Li, Phys. Rev. D **22**, 2860 (1980).
  - [19] R. Foot, H. Lew, X. G. He and G. C. Joshi, Z. Phys. C **44**, 441 (1989).
  - [20] A compilation of possible 1-loop structures for neutrino masses has been given in: E. Ma, Phys. Rev. Lett. **81**, 1171 (1998) [arXiv:hep-ph/9805219].
  - [21] A. Zee, Nucl. Phys. B **264** (1986) 99.
  - [22] K. S. Babu, Phys. Lett. B **203** (1988) 132.
  - [23] C. S. Aulakh and R. N. Mohapatra, Phys. Lett. B **119**, 136 (1982).
  - [24] L. J. Hall and M. Suzuki, Nucl. Phys. B **231**, 419 (1984).
  - [25] G. G. Ross and J. W. F. Valle, Phys. Lett. B **151**, 375 (1985).

- [26] M. Drees, S. Pakvasa, X. Tata and T. ter Veldhuis, Phys. Rev. D **57**, 5335 (1998) [arXiv:hep-ph/9712392].
- [27] H. K. Dreiner, J. Soo Kim and M. Thormeier, arXiv:0711.4315 [hep-ph].
- [28] H. K. Dreiner, C. Luhn, H. Murayama and M. Thormeier, Nucl. Phys. B **774**, 127 (2007) [arXiv:hep-ph/0610026].
- [29] H. K. Dreiner, C. Luhn and M. Thormeier, Phys. Rev. D **73**, 075007 (2006) [arXiv:hep-ph/0512163].
- [30] A. Masiero and J. W. F. Valle, Phys. Lett. **B251**, 273 (1990).
- [31] C. Amsler *et al.* [Particle Data Group], Phys. Lett. B **667**, 1 (2008).
- [32] E. J. Chun, S. K. Kang, C. W. Kim and U. W. Lee, Nucl. Phys. B **544**, 89 (1999) [arXiv:hep-ph/9807327].
- [33] For a review on  $R_p$  phenomenology, see for example: R. Barbier *et al.*, Phys. Rept. **420**, 1 (2005) [arXiv:hep-ph/0406039].
- [34] For a review on bilinear R-parity violation see, M. Hirsch and J. W. F. Valle, New J. Phys. **6**, 76 (2004) [arXiv:hep-ph/0405015].
- [35] R. Hempfling, Nucl. Phys. **B478**, 3 (1996).
- [36] M. Hirsch, M. A. Diaz, W. Porod, J. C. Romao and J. W. F. Valle, Phys. Rev. D **62**, 113008 (2000) [Erratum-ibid. D **65**, 119901 (2002)] [arXiv:hep-ph/0004115].
- [37] M. A. Diaz, M. Hirsch, W. Porod, J. C. Romao and J. W. F. Valle, Phys. Rev. D **68**, 013009 (2003) [Erratum-ibid. D **71**, 059904 (2005)] [arXiv:hep-ph/0302021].
- [38] W. Porod, M. Hirsch, J. Romao and J. W. F. Valle, Phys. Rev. D **63**, 115004 (2001) [arXiv:hep-ph/0011248].
- [39] M. Hirsch, W. Porod, J. C. Romao and J. W. F. Valle, Phys. Rev. D **66**, 095006 (2002) [arXiv:hep-ph/0207334].
- [40] M. Hirsch and W. Porod, Phys. Rev. D **68**, 115007 (2003) [arXiv:hep-ph/0307364].
- [41] H. K. Dreiner and S. Grab, arXiv:0811.0200 [hep-ph].
- [42] M. A. Bernhardt, S. P. Das, H. K. Dreiner and S. Grab, arXiv:0810.3423 [hep-ph].
- [43] H. K. Dreiner, S. Grab and M. K. Trenkel, Phys. Rev. D **79**, 016002 (2009) [arXiv:0808.3079 [hep-ph]].
- [44] B. C. Allanach, M. A. Bernhardt, H. K. Dreiner, C. H. Kom and P. Richardson, Phys. Rev. D **75**, 035002 (2007) [arXiv:hep-ph/0609263].
- [45] J. E. Kim and H. P. Nilles, Phys. Lett. B **138**, 150 (1984).
- [46] R. Barbieri, S. Ferrara and C. A. Savoy, Phys. Lett. **B119**, 343 (1982).
- [47] H. P. Nilles, M. Srednicki and D. Wyler, Phys. Lett. B **120**, 346 (1983).
- [48] A. Djouadi *et al.*, JHEP **0807**, 002 (2008) [arXiv:0801.4321 [hep-ph]].
- [49] U. Ellwanger and C. Hugonie, Comput. Phys. Commun. **175**, 290 (2006) [arXiv:hep-ph/0508022].
- [50] U. Ellwanger, J. F. Gunion and C. Hugonie, JHEP **0507**, 041 (2005) [arXiv:hep-ph/0503203].
- [51] D. E. Lopez-Fogliani and C. Munoz, Phys. Rev. Lett. **97**, 041801 (2006) [arXiv:hep-ph/0508297].
- [52] N. Escudero, D. E. Lopez-Fogliani, C. Munoz and R. R. de Austri, arXiv:0810.1507 [hep-ph].
- [53] P. Ghosh and S. Roy, arXiv:0812.0084 [hep-ph].
- [54] R. Kitano and K. y. Oda, Phys. Rev. D **61**, 113001 (2000) [arXiv:hep-ph/9911327].
- [55] A. Abada and G. Moreau, JHEP **0608**, 044 (2006) [arXiv:hep-ph/0604216].
- [56] M. Chemtob and P. N. Pandita, Phys. Rev. D **73**, 055012 (2006) [arXiv:hep-ph/0601159].
- [57] Y. Chikashige, R. N. Mohapatra and R. D. Peccei, Phys. Lett. B **98**, 265 (1981).
- [58] G. B. Gelmini and M. Roncadelli, Phys. Lett. B **99**, 411 (1981).
- [59] P. Skands *et al.*, JHEP **0407** (2004) 036 [arXiv:hep-ph/0311123].
- [60] B. Allanach *et al.*, Comput. Phys. Commun. **180** (2009) 8 [arXiv:0801.0045 [hep-ph]].
- [61] F. Franke and H. Fraas, Phys. Lett. B **353** (1995) 234 [arXiv:hep-ph/9504279].
- [62] D. J. Miller, R. Nevzorov and P. M. Zerwas, Nucl. Phys. B **681** (2004) 3 [arXiv:hep-ph/0304049].
- [63] J. C. Romao, M. A. Diaz, M. Hirsch, W. Porod and J. W. F. Valle, Phys. Rev. D **61** (2000) 071703 [arXiv:hep-ph/9907499].
- [64] M. Hirsch, H. V. Klapdor-Kleingrothaus and S. G. Kovalenko, Phys. Lett. B **398**, 311 (1997) [arXiv:hep-ph/9701253].
- [65] M. Hirsch, H. V. Klapdor-Kleingrothaus and S. G. Kovalenko, Phys. Rev. D **57**, 1947 (1998) [arXiv:hep-ph/9707207].
- [66] Y. Grossman and H. E. Haber, Phys. Rev. Lett. **78**, 3438 (1997) [arXiv:hep-ph/9702421].
- [67] J. A. Aguilar-Saavedra *et al.*, Eur. Phys. J. C **46**, 43 (2006) [arXiv:hep-ph/0511344].
- [68] B. C. Allanach *et al.*, in *Proc. of the APS/DPF/DPB Summer Study on the Future of Particle Physics (Snowmass 2001)* ed. N. Graf, *In the Proceedings of APS / DPF / DPB Summer Study on the Future of Particle Physics (Snowmass 2001)*, Snowmass, Colorado, 30 Jun - 21 Jul 2001, pp P125 [arXiv:hep-ph/0202233].
- [69] G. Aad *et al.* [The ATLAS Collaboration], [arXiv:0901.0512].
- [70] W. Porod, Comput. Phys. Commun. **153** (2003) 275 [arXiv:hep-ph/0301101].
- [71] D. F. Carvalho, M. E. Gomez and J. C. Romao, Phys. Rev. D **65**, 093013 (2002) [arXiv:hep-ph/0202054].
- [72] S. Schael *et al.* [ALEPH Collaboration and DELPHI Collaboration and L3 Collaboration and ], Eur. Phys. J. C **47** (2006) 547 [arXiv:hep-ex/0602042].
- [73] M. Hirsch, A. Vicente and W. Porod, Phys. Rev. D **77**, 075005 (2008) [arXiv:0802.2896 [hep-ph]].